Bulletin of Mathematical Biology (2020) 82:46
https://doi.org/10.1007/s11538-020-00722-1

Society for Mathematical Biology

ORIGINAL ARTICLE

Dynamic Analysis of the Time-Delayed Genetic Regulatory Network Between Two Auto-Regulated and Mutually Inhibitory Genes

Guiyuan Wang[1,2] · Zhuoqin Yang[1] · Marc Turcotte[3]

Received: 18 August 2019 / Accepted: 16 March 2020 / Published online: 31 March 2020

Abstract
Time delays play important roles in genetic regulatory networks. In this paper, a gene regulatory network model with time delays and mutual inhibition is considered, where time delays are regarded as bifurcation parameters. In the first part of this paper, we analyze the associated characteristic equations and obtain the conditions for the stability of the system and the existence of Hopf bifurcations in five special cases. Explicit formulas are given to determine the direction and stability of the Hopf bifurcation by using the normal form method and the center manifold theorem. Numerical simulations are then performed to illustrate the results we obtained. In the second part of the paper, using time-delayed stochastic numerical simulations, we study the impact of biological fluctuations on the system and observe that, in modest noise regimes, unexpectedly, noise acts to stabilize the otherwise destabilized oscillatory system.

Keywords Time delays · Hopf bifurcation · Oscillation · Stability · Genetic regulatory network model · Noise

1 Introduction

Genetic regulatory networks (GRNs) describe interactions between DNA, RNA, proteins and small molecules in living cells and play fundamental roles in many life

✉ Marc Turcotte
marc.turcotte@utdallas.edu

Zhuoqin Yang
yangzhuoqin@buaa.edu.cn

1 School of Mathematics and Systems Science and LMIB, Beihang University, Beijing 100191, China

2 College of Sciences, Hebei University of Science and Technology, Shijiazhuang 050018, Hebei, P.R. China

3 Biological Sciences Department, The University of Texas at Dallas, Richardson, TX 75080, USA

processes (Parmar et al. 2015; Ling et al. 2017). Because the processes of gene transcription and messenger RNA translation are not co-located in space and consequently not completed instantaneously, time delays are inevitable in GRNs. The effect of time delay on the dynamic behavior of a GRN model has attracted extensive attention of many scholars, and some research results have been obtained (Parmar et al. 2015; Ling et al. 2017; Wu and Eshete 2011; Bodnar and Bartłomiejczyk 2012; Lewis 2003; Wu 2011; Wang et al. 2010; Wu 2011; Zhang et al. 2017; Lai 2018; Monk 2003; Verdugo and Rand 2008; Sun et al. 2018; Yue et al. 2017; Huang et al. 2016). In Wu and Eshete (2011), the authors considered a model of gene express with two delays and showed effect of time delays on the model. In Bodnar and Bartłomiejczyk (2012), the Hes 1 genetic oscillator system was presented, and the authors showed that the stability of the steady state depends on the sum of time delays. The conditions for the occurrence of Hopf bifurcation and the stability of equilibrium point were proved. Zhang et al. (2017) investigated oscillatory expression in Escherichia coli. The result of their research indicates that the effects of transcriptional and translational delays are two important factors for designing or controlling GRNs and that the effect of diffusion must be taken into account. In Lai (2018), the stability and bifurcation of delayed bidirectional GRNs with negative feedback loops were invested.

In recent years, the cyclic GRNs (CGRNs) have attracted the attention of scholars, and many research results have been achieved (Lewis 2003; Wu 2011; Qiu 2010; Bar-Or et al. 2000; Ling et al. 2015). CGRNs are a kind of GRNs. All the nodes of CGRNs are arranged in a ring structure. In Lewis (2003), Lewis showed, using mathematical simulation, that the direct auto-repression of a gene by its own product could generate oscillations. The period of oscillation was found to be determined by the transcriptional and translational delay. In Wu (2011), Wu first presented conditions for delay-independent local stability of CGRNs and then proceeded to study the bifurcation of ring-structured GRNs with time delays. In Ling et al. (2015), the stability and bifurcation of CGRNs with mixed time delays were studied. Due to the presence of time delays, even if the GRN model is simple, a positive equilibrium point of the system will lose its stability. Sustainable periodic oscillation will occur through a Hopf bifurcation (Parmar et al. 2015; Suzuki et al. 2016). Delay is not considered in the CGRN models in Xi and Turcotte (2015). We consider the effect of time delay on the canonical two-gene binary switch model (see Fig. 1), which is described by the following delay differential equations.

$$\begin{cases} M'_1(t) = -r_1 M_1(t) + a \cdot a_1 \frac{P_1^n(t-\tau_2)}{s^n + P_1^n(t-\tau_2)} + b \cdot b_{21} \frac{s^n}{s^n + P_2^n(t-\tau_2)} \\ M'_2(t) = -r_2 M_2(t) + a \frac{P_2^n(t-\tau_2)}{s^n + P_2^n(t-\tau_2)} + b \frac{s^n}{s^n + P_1^n(t-\tau_2)} \\ P'_1(t) = -c_1 P_1(t) + d_1 M_1(t-\tau_1) \\ P'_2(t) = -c_2 P_2(t) + d_2 M_2(t-\tau_1) \end{cases} \tag{1}$$

Let $\tau = \max\{\tau_1, \tau_2\}$ and then the initial conditions of the model are given by:

$$M_1(s) = \phi_1(s), \quad M_2(s) = \phi_2(s), \quad P_1(s) = \phi_3(s), \quad P_2(s) = \phi_4(s),$$

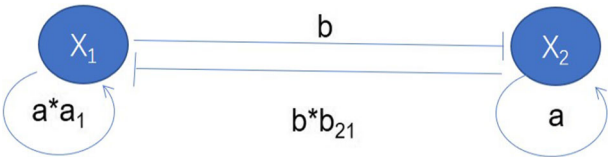

Fig. 1 Two-gene mutually repressive, self-promoting model (Xi and Turcotte 2015). The nodes are genes X_1 and X_2. Parameter asymmetry provider bcommon $= b_{21}$

where $s \in [-\tau, 0], \phi_i(s) \in C([-\tau, 0], R)$ $(i = 1, 2, 3, 4, \phi_i(s) \geq 0)$. Here $C([-\tau, 0], R)$ is the Banach space. $M_i(t)$ $(i = 1, 2)$ and $P_i(t)$ $(i = 1, 2)$ describe the concentration of mRNA and protein of genes X_1 and X_2, respectively. r_i $(i = 1, 2)$ and c_i $(i = 1, 2)$ are degradation rates of mRNA and protein, respectively. d_i $(i = 1, 2)$ are translation rates. Parameters a and b are transcription rates, n is the Hill coefficient. a_1 and bcommon are parameter asymmetry providers. All the parameters of the model are positive real numbers.

The organization of the paper is as follows: In Sect. 2, we study the stability and existence of Hopf bifurcation of system (1) in five cases. The explicit formula is given to determine the direction and stability of bifurcating periodic solutions by using the normal form method and the center manifold theorem in Sect. 3. In Sect. 4, numerical simulations are presented that support the analytical results we obtained. In Sect. 5, using time-delayed stochastic simulations, we study the impact of biological fluctuations (noise) on the dynamics of the system. In Sect. 6, characterization of the orbit is discussed. Finally, in Sect. 7, we discuss the significance of our results and present our conclusions.

2 The Stability and Existence of Hopf Bifurcation

Let $E_* = E(M_1^*, M_2^*, P_1^*, P_2^*)$ be the positive equilibrium of system (1), then

$$\begin{cases} -r_1 M_1^* + a \cdot a_1 \frac{(P_1^*)^n}{s^n + (P_1^*)^n} + b \cdot b_{21} \frac{s^n}{s^n + (P_2^*)^n} = 0, \\ -r_2 M_2^* + a \frac{(P_2^*)^n}{s^n + (P_2^*)^n} + b \frac{s^n}{s^n + (P_1^*)^n} = 0, \\ -c_1 P_1^* + d_1 M_1^* = 0, \\ -c_2 P_2^* + d_2 M_2^* = 0. \end{cases}$$

Thus, we can get E_*, where $P_1^*, M_1^*, P_2^*, M_2^*$ are defined in Appendix.

By the linear transform,

$$u_1(t) = M_1(t) - M_1^*, \quad u_2(t) = M_2(t) - M_2^*, \quad u_3(t) = P_1(t) - P_1^*,$$
$$u_4(t) = P_2(t) - P_2^*$$

We have

$$\begin{cases} \dot{u}_1(t) = a_{11}u_1(t) + a_{13}u_3(t-\tau_2) + a_{14}u_4(t-\tau_2) + F_1, \\ \dot{u}_2(t) = a_{22}u_2(t) + a_{23}u_3(t-\tau_2) + a_{24}u_4(t-\tau_2) + F_2, \\ \dot{u}_3(t) = a_{31}u_1(t-\tau_1) + a_{33}u_3(t) + F_3, \\ \dot{u}_4(t) = a_{42}u_2(t-\tau_1) + a_{44}u_4(t) + F_4, \end{cases} \tag{2}$$

where

$$f^{(1)} = -r_1 M_1 + a \cdot a_1 \frac{P_1^n(t-\tau_2)}{s^n + P_1^n(t-\tau_2)} + b \cdot b_{21} \frac{s^n}{s^n + P_2^n(t-\tau_2)},$$

$$f^{(2)} = -r_2 M_2 + a \frac{P_2^n(t-\tau_2)}{s^n + P_2^n(t-\tau_2)} + b \frac{s^n}{s^n + P_1^n(t-\tau_2)},$$

$$f^{(3)} = -c_1 P_1(t) + d_1 M_1(t-\tau_1),$$

$$f^{(4)} = -c_2 P_2(t) + d_2 M_2(t-\tau_1),$$

$$f_{ijk}^{(1)} = \left. \frac{\partial^{i+j+k} f^{(1)}}{\partial M_1^i(t)\, \partial P_1^j(t-\tau_2) \partial P_2^k(t-\tau_2)} \right|_{(M_1^*, M_2^*, P_1^*, P_2^*)}, \quad i, j, k \geq 0,$$

$$f_{ijk}^{(2)} = \left. \frac{\partial^{i+j+k} f^{(2)}}{\partial M_2^i(t)\, \partial P_1^j(t-\tau_2) \partial P_2^k(t-\tau_2)} \right|_{(M_1^*, M_2^*, P_1^*, P_2^*)}, \quad i, j, k \geq 0,$$

$$f_{ij}^{(3)} = \left. \frac{\partial^{i+j} f^{(3)}}{\partial M_1^i(t-\tau_1)\, \partial P_1^j(t)} \right|_{(M_1^*, M_2^*, P_1^*, P_2^*)}, \quad i, j \geq 0,$$

$$f_{ij}^{(4)} = \left. \frac{\partial^{i+j} f^{(4)}}{\partial M_2^i(t-\tau_1)\, \partial P_2^j(t)} \right|_{(M_1^*, M_2^*, P_1^*, P_2^*)}, \quad i, j \geq 0,$$

$$F_1 = \sum_{i+j+k \geq 2} \frac{1}{i!j!k!} f_{ijk}^{(1)} u_1^i(t)\, u_3^j(t-\tau_2)\, u_4^k(t-\tau_2),$$

$$F_2 = \sum_{i+j+k \geq 2} \frac{1}{i!j!k!} f_{ijk}^{(2)} u_2^i(t)\, u_3^j(t-\tau_2)\, u_4^k(t-\tau_2),$$

$$F_3 = \sum_{i+j \geq 2} \frac{1}{i!j!} f_{ij}^{(3)} u_1^i(t-\tau_1)\, u_3^j(t),$$

$$F_4 = \sum_{i+j \geq 2} \frac{1}{i!j!} f_{ij}^{(4)} u_2^i(t-\tau_1)\, u_4^j(t),$$

$$a_{11} = -r_1, \quad a_{12} = 0, \quad a_{13} = \frac{a a_{11} n \left(P_1^*\right)^{n-1} s^n}{\left(s^n + \left(P_1^*\right)^n\right)^2}, \quad a_{14} = -\frac{b b_{21} n \left(P_2^*\right)^{n-1} s^n}{\left(s^n + \left(P_2^*\right)^n\right)^2},$$

$$a_{21} = 0, \quad a_{22} = -r_2, \quad a_{23} = -\frac{b n \left(P_1^*\right)^{n-1} s^n}{\left(s^n + \left(P_1^*\right)^n\right)^2}, \quad a_{24} = \frac{a n \left(P_2^*\right)^{n-1} s^n}{\left(s^n + \left(P_2^*\right)^n\right)^2},$$

$$a_{31} = d_1, \quad a_{32} = 0, \quad a_{33} = -c_1, \quad a_{34} = 0,$$
$$a_{41} = 0, \quad a_{42} = d_2, \quad a_{43} = 0, \quad a_{44} = -c_2.$$

Then the linear part of system (2) is

$$\begin{cases} \dot{u}_1(t) = a_{11}u_1(t) + a_{13}u_3(t-\tau_2) + a_{14}u_4(t-\tau_2), \\ \dot{u}_2(t) = a_{22}u_2(t) + a_{23}u_3(t-\tau_2) + a_{24}u_4(t-\tau_2), \\ \dot{u}_3(t) = a_{31}u_1(t-\tau_1) + a_{33}u_3(t), \\ \dot{u}_4(t) = a_{42}u_2(t-\tau_1) + a_{44}u_4(t). \end{cases} \tag{3}$$

Thus, the characteristic equation of system (3) is obtained:

$$\det \begin{bmatrix} \lambda - a_{11} & 0 & -a_{13}e^{-\lambda\tau_2} & -a_{14}e^{-\lambda\tau_2} \\ 0 & \lambda - a_{22} & -a_{23}e^{-\lambda\tau_2} & -a_{24}e^{-\lambda\tau_2} \\ -a_{31}e^{-\lambda\tau_1} & 0 & \lambda - a_{33} & 0 \\ 0 & -a_{42}e^{-\lambda\tau_1} & 0 & \lambda - a_{44} \end{bmatrix} = 0$$

which is equivalent to

$$\lambda^4 + A_3\lambda^3 + A_2\lambda^2 + A_1\lambda + A_0 + (B_2\lambda^2 + B_1\lambda + B_0)e^{-\lambda(\tau_1+\tau_2)} + C_0e^{-2\lambda(\tau_1+\tau_2)} = 0 \tag{4}$$

where

$$\begin{aligned} A_0 &= a_{11}a_{22}a_{33}a_{44}, \\ A_1 &= -(a_{11}a_{33}a_{44} + a_{22}a_{33}a_{44} + a_{11}a_{22}a_{44} + a_{11}a_{22}a_{33}), \\ A_2 &= a_{44}(a_{11} + a_{22} + a_{33}) + a_{22}(a_{11} + a_{33}) + a_{11}a_{33}, \\ A_3 &= -(a_{11} + a_{22} + a_{33} + a_{44}), \\ B_0 &= -(a_{31}a_{13}a_{22}a_{44} + a_{11}a_{42}a_{24}a_{33}), \\ B_1 &= a_{42}a_{24}a_{33} + a_{31}a_{13}(a_{44} + a_{22}) + a_{11}a_{42}a_{24}, \\ B_2 &= -(a_{42}a_{24} + a_{31}a_{13}), \\ C_0 &= a_{31}a_{42}a_{13}a_{24} - a_{31}a_{42}a_{14}a_{23}. \end{aligned}$$

From the form of Eq. (4), it is explicitly clear that the system's stability depends on the sum of the delays. For Eq. (4), we consider the following five cases.

Case 1 $\tau = \tau_1 + \tau_2 = 0$ (i.e., $\tau_1 = \tau_2 = 0$).

Equation (4) reduces to

$$\lambda^4 + A_3\lambda^3 + (A_2 + B_2)\lambda^2 + (A_1 + B_1)\lambda + A_0 + B_0 + C_0 = 0 \tag{5}$$

By the Routh–Hurwitz criteria, all the roots of Eq. (5) have negative real parts if and only if

$$V_1 = A_3 > 0, \tag{6}$$

$$V_2 = \begin{vmatrix} A_3 & 1 \\ A_1 + B_1 & A_2 + B_2 \end{vmatrix} = A_3 (A_2 + B_2) - A_1 - B_1 > 0, \tag{7}$$

$$V_3 = \begin{vmatrix} A_3 & 1 & 0 \\ A_1 + B_1 & A_2 + B_2 & A_3 \\ 0 & A_0 + B_0 + C_0 & A_1 + B_1 \end{vmatrix} > 0, \tag{8}$$

$$V_4 = \begin{vmatrix} A_3 & 1 & 0 & 0 \\ A_1 + B_1 & A_2 + B_2 & A_3 & 1 \\ 0 & A_0 + B_0 + C_0 & A_1 + B_1 & A_2 + B_2 \\ 0 & 0 & 0 & A_0 + B_0 + C_0 \end{vmatrix} > 0. \tag{9}$$

Then system (1) is stable at E_*. If $A_0 + B_0 + C_0 \neq 0$, Eq. (5) has no zero roots. Hence, the fold bifurcation does not occur.

Case 2 $\tau = \tau_1 + \tau_2 > 0$.

Equation (4) becomes

$$\begin{aligned} &\lambda^4 + A_3\lambda^3 + A_2\lambda^2 + A_1\lambda + A_0 \\ &\quad + (B_2\lambda^2 + B_1\lambda + B_0)e^{-\lambda\tau} + C_0 e^{-2\lambda\tau} = 0. \end{aligned} \tag{10}$$

We take the time delay $\tau = \tau_1 + \tau_2$ as bifurcation parameters and investigate dynamics of system (1).

$i\omega$ ($\omega > 0$) is the root of Eq. (10) if and only if $i\omega$ satisfies

$$\begin{cases} \left(\omega^4 - A_2\omega^2 + A_0 + C_0\right)\cos(\omega\tau) + \left(A_3\omega^3 - A_1\omega\right)\sin(\omega\tau) = B_2\omega^2 - B_0 \\ \left(A_1\omega - A_3\omega^3\right)\cos(\omega\tau) + \left(\omega^4 - A_2\omega^2 + A_0 - C_0\right)\sin(\omega\tau) = -B_1\omega \end{cases} \tag{11}$$

By Eq. (11), we get

$$\cos(\omega\tau) = \frac{e_5\omega^6 + e_6\omega^4 + e_7\omega^2 + e_8}{\omega^8 + e_1\omega^6 + e_2\omega^4 + e_3\omega^2 + e_4},$$

$$sin(\omega\tau) = \frac{\omega\left(e_9\omega^4 + e_{10}\omega^2 + e_{11}\right)}{\omega^8 + e_1\omega^6 + e_2\omega^4 + e_3\omega^2 + e_4},$$

where

$$\begin{aligned} e_1 &= A_3^2 - 2A_2, \\ e_2 &= A_2^2 - 2A_1A_3 + 2A_0, \\ e_3 &= A_1^2 - 2A_0A_2, \end{aligned}$$

$$
\begin{aligned}
e_4 &= {A_0}^2 - {C_0}^2,\\
e_5 &= B_2,\\
e_6 &= B_1A_3 - A_2B_2 - B_0,\\
e_7 &= A_2B_0 + A_0B_2 - A_1B_1 - C_0B_2,\\
e_8 &= C_0B_0 - A_0B_0,\\
e_9 &= A_3B_2 - B_1,\\
e_{10} &= A_2B_1 - A_3B_0 - A_1B_2,\\
e_{11} &= A_1B_0 - C_0B_1 - A_0B_1.
\end{aligned}
$$

Since $\cos^2(\omega\tau) + sin^2(\omega\tau) = 1$, we obtain

$$\omega^{16} + k_7\omega^{14} + k_6\omega^{12} + k_5\omega^{10} + k_4\omega^8 + k_3\omega^6 + k_2\omega^4 + k_1\omega^2 + k_0 = 0 \quad (12)$$

where

$$
\begin{aligned}
k_0 &= {e_4}^2 - {e_8}^2,\\
k_1 &= 2e_3e_4 - 2e_7e_8 - {e_{11}}^2,\\
k_2 &= {e_3}^2 - 2e_{10}e_{11} + 2e_2e_4 - 2e_6e_8 - {e_7}^2,\\
k_3 &= 2e_2e_3 - 2e_9e_{11} - 2e_6e_7 - {e_{10}}^2 - 2e_5e_8 + 2e_1e_4,\\
k_4 &= {e_2}^2 + 2e_1e_3 - 2e_5e_7 - 2e_9e_{10} + 2e_4 - {e_6}^2,\\
k_5 &= 2e_3 + 2e_1e_2 - 2e_5e_6 - {e_9}^2,\\
k_6 &= {e_1}^2 + 2e_2 - {e_5}^2,\\
k_7 &= 2e_1.
\end{aligned}
$$

Denote $z = \omega^2$, then Eq. (12) becomes

$$z^8 + k_7z^7 + k_6z^6 + k_5z^5 + k_4z^4 + k_3z^3 + k_2z^2 + k_1z + k_0 = 0 \quad (13)$$

Let $h(z) = z^8 + k_7z^7 + k_6z^6 + k_5z^5 + k_4z^4 + k_3z^3 + k_2z^2 + k_1z + k_0$, it is obvious Eq. (13) has no positive root if $k_i > 0, i = 0 \ldots 7$. It means that system (1) is stable for all $\tau \geq 0$. On the other hand, since $\lim_{z\to\infty} h(z) = +\infty$, we know that Eq. (13) has at least one positive root if $k_0 < 0$. Without loss of generality, we assume that it has eight positive real roots, defined by $z_k, k = 1, \ldots 8$, respectively. From Eq. (11), we have

$$\cos(\omega_k\tau_k) = \frac{e_5\omega_k^6 + e_6\omega_k^4 + e_7\omega_k^2 + e_8}{\omega_k^8 + e_1\omega_k^6 + e_2\omega_k^4 + e_3\omega_k^2 + e_4}.$$

It follows that

$$\tau_k^j = \frac{1}{\omega_k}\arccos\left(\frac{e_5\omega_k^6 + e_6\omega_k^4 + e_7\omega_k^2 + e_8}{\omega_k^8 + e_1\omega_k^6 + e_2\omega_k^4 + e_3\omega_k^2 + e_4}\right) + \frac{2j\pi}{\omega_k},$$

where $k = 1, \ldots 8$; $j = 0, 1 \ldots$.

Define

$$\tau_0 = \tau_{k_0} = \min_{k\in\{1,\ldots,8\}} \left\{\tau_k^0\right\}, \quad \omega_0 = \omega_{k_0}.$$

For convenience, let

$$\bigcup_{k=1}^{8} \left\{\tau_k^j\right\}_{j=0}^{+\infty} = \{\tau_i\}_{i=0}^{+\infty} \tag{14}$$

such that

$$\tau_0 < \tau_1 < \tau_2 < \cdots < \tau_j < \cdots \tag{15}$$

Multiplying $e^{\lambda\tau}$ on both sides of Eq. (10) and taking the derivative of $\lambda(\tau)$ with respect to τ, we get

$$\begin{aligned}
&\operatorname{sgn}\left[\operatorname{Re}\left(\frac{d\lambda(\tau)}{d\tau}\right)_{\tau=\tau_0}\right] \\
&= \operatorname{sgn}\left\{\left[\operatorname{Re}\left(\frac{d\lambda(\tau)}{d\tau}\right)^{-1}\right]_{\tau=\tau_0}\right\} \\
&= \operatorname{sgn}\left(\operatorname{Re}\left(\frac{\left(4\lambda^3 + 3A_3\lambda^2 + 2A_2\lambda + A_1\right)e^{\lambda\tau} + 2B_2\lambda + B_1}{C_0\lambda e^{-\lambda\tau} - \left(\lambda^4 + A_3\lambda^3 + A_2\lambda^2 + A_1\lambda + A_0\right)\lambda e^{\lambda\tau}} - \frac{\tau}{\lambda}\right)_{\tau=\tau_0}\right) \\
&= \operatorname{sgn}\left(\frac{P_1P_3 + P_2P_4}{{P_1}^2 + {P_2}^2}\right),
\end{aligned}$$

where

$$\begin{aligned}
P_1 &= 2C_0\sin(\omega_0\tau_0) - B_1\omega_0^2, \\
P_2 &= B_0\omega_0 - B_2\omega_0^3 + 2C_0\omega_0\cos(\omega_0\tau_0), \\
P_3 &= \left(A_1 - 3A_3\omega_0^2\right)\cos(\omega_0\tau_0) + \left(4\omega_0^3 - 2A_2\omega_0\right)\sin(\omega_0\tau_0) + B_1, \\
P_4 &= \left(2A_2\omega_0 - 4\omega_0^3\right)\cos(\omega_0\tau_0) + \left(A_1 - 3A_3\omega_0^2\right)\sin(\omega_0\tau_0) + 2B_2\omega_0.
\end{aligned}$$

If condition (H3) $P_1P_3 + P_2P_4 \neq 0$ holds, then $\operatorname{Re}\left(\frac{d\lambda(\tau)}{d\tau}\right)^{-1}_{\tau=\tau_0} \neq 0$.

In order to obtain our main results, it is necessary to give the following conditions.

(H1) Formulas (6)–(9) hold;
(H2) Equation (13) has at least one positive real root;
(H3) $P_1P_3 + P_2P_4 \neq 0$.

In summary, we have the following results.

Theorem 1 *For system* (1)*, the following results hold.*

(i) *If* $k_i > 0, i = 0 \ldots 7$, $A_0 + B_0 + C_0 \neq 0$ *and (H1) hold, then the positive equilibrium* E_* *is asymptotically stable for all* $\tau \geq 0$*. In other words, Hopf bifurcation does not occur for all* $\tau \geq 0$.

(ii) *If conditions (H1), (H2) and (H3) hold, then the positive equilibrium* E_* *of System* (1) *is asymptotically stable when* $0 \leq \tau < \tau_0$ *and unstable when* $\tau > \tau_0$*. Furthermore, System* (1) *undergoes a Hopf bifurcation at* E_* *when* $\tau = \tau_j$, $j = 0, 1, 2, \ldots$.

Proof (i) When $\tau = 0$, characteristic Eq. (10) becomes

$$\lambda^4 + A_3\lambda^3 + (A_2 + B_2)\lambda^2 + (A_1 + B_1)\lambda + A_0 + B_0 + C_0 = 0.$$

According to Routh–Hurwitz criterion, all the roots of above equation have negative real parts if and only if (H1) holds. Hence, all the roots of Eq. (10) have negative real parts when $\tau = 0$.

On the other hand, from $k_i > 0, i = 0 \ldots 7$, we obtain $h(0) = k_0 > 0$ and $h'(z) = 8z^7 + 7k_7z^6 + 6k_6z^5 + 5k_5z^4 + 4k_4z^3 + 3k_3z^2 + 2k_2z + k_1$. Thus, we have Eq. (13) has no real root, and hence Eq. (10) has no purely imaginary root. Since $A_0 + B_0 + C_0 \neq 0$, $\lambda = 0$ is not a root of Eq. (10). To sum up, we can obtain that Eq. (10) has no root with zero real part for all $\tau > 0$. Therefore, all the roots of Eq. (10) have negative real parts for all $\tau \geq 0$. This completes the proof of (i).

(ii) The definition of τ_0 implies that all the roots of Eq. (10) have negative real parts when $0 \leq \tau < \tau_0$. Hence, the positive equilibrium E_* is asymptotically stable for $0 \leq \tau < \tau_0$. If the condition (H2) holds, Eq. (13) has at least one real root, which indicates that the positive equilibrium E_* is unstable for $\tau > \tau_0$. Moreover, $P_1P_3 + P_2P_4 \neq 0$ implies that the transversality condition for Hopf bifurcations is satisfied under the given assumption (H3). Therefore, System (1) undergoes a Hopf bifurcation at E_* when $\tau = \tau_j$, $j = 0, 1, 2, \ldots$.

Case 3 $\tau_2 > 0, \tau_1 = 0$. Equation (4) becomes

$$\lambda^4 + A_3\lambda^3 + A_2\lambda^2 + A_1\lambda + A_0 + (B_2\lambda^2 + B_1\lambda + B_0)e^{-\lambda\tau_2} + C_0e^{-2\lambda\tau_2} = 0$$

It is same as the characteristic equation in case 2, and similar results can be obtained. The difference is that case 2 takes the sum of time delays as the bifurcation parameter. Here, only the time delay τ_2 is used as the bifurcation parameter. For the case $\tau_1 > 0, \tau_2 = 0$, with τ_1 as the bifurcation parameter, the characteristic equation remains unchanged, and similar results will be obtained.

Case 4 $\tau_1 = \tau_2 = \tau \neq 0$. Equation (4) becomes

$$\lambda^4 + A_3\lambda^3 + A_2\lambda^2 + A_1\lambda + A_0 + (B_2\lambda^2 + B_1\lambda + B_0)e^{-2\lambda\tau} + C_0e^{-4\lambda\tau} = 0 \quad (16)$$

$i\omega\,(\omega > 0)$ is the root of Eq. (16) if and only if $i\omega$ satisfies

$$\begin{cases} \left(\omega^4 - A_2\omega^2 + A_0 + C_0\right)\cos(2\omega\tau) + \left(A_3\omega^3 - A_1\omega\right)\sin(2\omega\tau) = B_2\omega^2 - B_0 \\ \left(A_1\omega - A_3\omega^3\right)\cos(2\omega\tau) + \left(\omega^4 - A_2\omega^2 + A_0 - C_0\right)\sin(2\omega\tau) = -B_1\omega \end{cases} \tag{17}$$

By Eq. (17), we get

$$\begin{aligned} \cos(2\omega\tau) &= \frac{e_5\omega^6 + e_6\omega^4 + e_7\omega^2 + e_8}{\omega^8 + e_1\omega^6 + e_2\omega^4 + e_3\omega^2 + e_4}, \\ sin(2\omega\tau) &= \frac{\omega\left(e_9\omega^4 + e_{10}\omega^2 + e_{11}\right)}{\omega^8 + e_1\omega^6 + e_2\omega^4 + e_3\omega^2 + e_4}. \end{aligned} \tag{18}$$

Since $\cos^2(2\omega\tau) + sin^2(2\omega\tau) = 1$, we get

$$\omega^{16} + k_7\omega^{14} + k_6\omega^{12} + k_5\omega^{10} + k_4\omega^8 + k_3\omega^6 + k_2\omega^4 + k_1\omega^2 + k_0 = 0 \tag{19}$$

Denote $z = \omega^2$, then Eq. (19) becomes

$$z^8 + k_7z^7 + k_6z^6 + k_5z^5 + k_4z^4 + k_3z^3 + k_2z^2 + k_1z + k_0 = 0 \tag{20}$$

This equation is the same as the case two.

Similar to case 2, we know that Eq. (20) has at least one positive root if $k_0 < 0$. Without loss of generality, we assume that it has eight positive real roots, defined by $z_k, k = 1, 2, \ldots, 8$, respectively. From (18), we have

$$\tau_k^j = \frac{1}{2\omega_k}\arccos\left(\frac{e_5\omega_k^6 + e_6\omega_k^4 + e_7\omega_k^2 + e_8}{\omega_k^8 + e_1\omega_k^6 + e_2\omega_k^4 + e_3\omega_k^2 + e_4}\right) + \frac{j\pi}{\omega_k} \tag{21}$$

where $k = 1, \ldots 8$; $j = 0, 1 \ldots$.

Define

$$\tau_0 = \tau_{k_0} = \min_{k\in\{1,\ldots,8\}}\left\{\tau_k^0\right\}, \omega_0 = \omega_{k_0}.$$

For convenience, let

$$\bigcup_{k=1}^{8}\left\{\tau_k^j\right\}_{j=0}^{+\infty} = \{\tau_i\}_{i=0}^{+\infty} \tag{22}$$

such that

$$\tau_0 < \tau_1 < \tau_2 < \cdots < \tau_j < \cdots \tag{23}$$

Multiplying $e^{2\lambda\tau}$ on both sides of Eq. (16) and taking the derivative of $\lambda(\tau)$ with respect to τ, we have

$$\begin{aligned}
&\operatorname{sgn}\left[\operatorname{Re}\left(\frac{d\lambda(\tau)}{d\tau}\right)_{\tau=\tau_0}\right] \\
&= \operatorname{sgn}\left\{\left[\operatorname{Re}\left(\frac{d\lambda(\tau)}{d\tau}\right)^{-1}\right]_{\tau=\tau_0}\right\} \\
&= \operatorname{sgn}\left(\operatorname{Re}\left(\frac{\left(4\lambda^3+3A_3\lambda^2+2A_2\lambda+A_1\right)e^{2\lambda\tau}+2B_2\lambda+B_1}{2C_0\lambda e^{-2\lambda\tau}-2\left(\lambda^4+A_3\lambda^3+A_2\lambda^2+A_1\lambda+A_0\right)\lambda e^{2\lambda\tau}}-\frac{\tau}{\lambda}\right)_{\tau=\tau_0}\right) \\
&= \operatorname{sgn}\left(\frac{Q_1Q_3+Q_2Q_4}{{Q_1}^2+{Q_2}^2}\right).
\end{aligned}$$

where

$$\begin{aligned}
x &= \cos(2\omega_0\tau_0), \\
y &= \sin(2\omega_0\tau_0), \\
Q_1 &= 2\omega_0\left(C_0y-\omega_0^4y-\omega_0^3A_3x-\omega_0^2A_2y+\omega_0A_1x+A_0y\right), \\
Q_2 &= 2\omega_0\left(C_0x-\omega_0^4x-\omega_0^3A_3y+\omega_0^2A_2x+\omega_0A_1y-A_0x\right), \\
Q_3 &= 4\omega_0^3y-3A_3\omega_0^2x-2A_2\omega_0y+A_1x+B_1, \\
Q_4 &= -4\omega_0^3x-3A_3\omega_0^2y+2A_2\omega_0x+A_1y+2B_2\omega_0.
\end{aligned}$$

If condition (H4) $Q_1Q_3+Q_2Q_4\neq 0$ holds, then $\operatorname{Re}\left(\frac{d\lambda(\tau)}{d\tau}\right)^{-1}_{\tau=\tau_0}\neq 0$. In order to obtain the main results, we give the following assumption.

(H4) $Q_1Q_3+Q_2Q_4\neq 0$;
(H5) Equation (20) has at least one positive real root.

Applying Hopf bifurcation theorem in Hassard et al. (1981), we have the following result. □

Theorem 2 *For System (1), suppose that (H1), (H4) and (H5) hold, then the positive equilibrium E_* of System (1) is asymptotically stable for $0\le\tau<\tau_0$ and unstable for $\tau>\tau_0$. Furthermore, System(1) undergoes a Hopf bifurcation at E_* when $\tau=\tau_j$, $j=0,1,2,\ldots$, where $\tau=\tau_j$ as defined in (23).*

Case 5 $\tau_2>0$, $\tau_1\in[0,\tau_{10})$,and $\tau_1\neq\tau_2$.

We consider Eq. (4) with τ_1 in its stable interval; τ_2 is regarded as a bifurcation parameter, where τ_{10} is the first bifurcation point when $\tau_2=0$. $i\omega_2$ $(\omega_2>0)$ is the root of Eq. (4) if and only if $i\omega_2$ satisfies

$$\begin{cases}
E_{11}\cos(\omega_2\tau_2)+E_{12}\sin(\omega_2\tau_2)=E_{13}, \\
E_{14}\cos(\omega_2\tau_2)+E_{15}\sin(\omega_2\tau_2)=E_{16},
\end{cases} \tag{24}$$

where

$$
\begin{aligned}
E_{11} &= {\omega_2}^4 - A_2{\omega_2}^2 + A_0 + C_0,\\
E_{12} &= A_3{\omega_2}^3 - A_1\omega_2,\\
E_{13} &= \left(B_2{\omega_2}^2 - B_0\right)\cos\left(\omega_2\tau_1\right) - B_1\omega_2 sin\left(\omega_2\tau_1\right),\\
E_{14} &= A_1\omega_2 - A_3{\omega_2}^3,\\
E_{15} &= {\omega_2}^4 - A_2{\omega_2}^2 + A_0 - C_0,\\
E_{16} &= -B_1\omega_2\cos\left(\omega_2\tau_1\right) + \left(B_0 - B_2{\omega_2}^2\right) sin\left(\omega_2\tau_1\right).
\end{aligned}
$$

From Eq. (24), we get

$$
\begin{aligned}
\cos\left(\omega_2\tau_2\right) &= -\frac{E_{12}E_{16} - E_{13}E_{15}}{E_{11}E_{15} - E_{14}E_{12}},\\
sin\left(\omega_2\tau_2\right) &= \frac{E_{11}E_{16} - E_{14}E_{13}}{E_{11}E_{15} - E_{14}E_{12}}.
\end{aligned}
\tag{25}
$$

From (25), we obtain

$$
\begin{aligned}
&{\omega_2}^{16} + n_1{\omega_2}^{14} + n_2{\omega_2}^{12} + n_3{\omega_2}^{10} + n_4{\omega_2}^8 + n_5{\omega_2}^6 + n_6{\omega_2}^4 + n_7{\omega_2}^2 + n_8\\
&+\left(m_0 + m_2{\omega_2}^2 + m_4{\omega_2}^4 + m_6{\omega_2}^6 + m_8{\omega_2}^8\right)\cos^2\left(\omega_2\tau_1\right)\\
&+\left(m_1\omega_2 + m_3{\omega_2}^3 + m_5{\omega_2}^5 + m_7{\omega_2}^7\right) sin\left(2\omega_2\tau_1\right) = 0,
\end{aligned}
\tag{26}
$$

where $n_i\ (i = 1\ldots 8)$, $m_j\ (j = 0\ldots 8)$ are defined in Appendix.

In order to get the main result, we give the following assumption.

(H6) Equation (26) has at least finite positive roots, defined by $\omega_2^{(1)}, \omega_2^{(2)}, \ldots \omega_2^{(k)}$. For every fixed $\omega_2^{(i)}$, $i = 1, 2\ldots k$, there exists a sequence τ_{2i}^j such that Eq. (26) holds.

From (25), we have

$$
\tau_{2i}^j = \frac{1}{\omega_2^{(i)}}\arccos\left(\frac{E_{13}E_{15} - E_{12}E_{16}}{E_{11}E_{15} - E_{14}E_{12}}\right) + \frac{2\pi j}{\omega_2^{(i)}}
$$

where $i = 1, 2\ldots k;\ j = 0, 1, 2, \ldots$.

Define

$$
\tau_{20} = \min\left\{\tau_{2i}^0\,|i = 1, 2, ..., k;\ j = 0, 1, 2, ...\right\}
$$

Therefore, Eq. (26) has a pair of purely imaginary roots $\pm i\omega_{20}$ when $\tau_2 = \tau_{20}$. Multiplying $e^{\lambda\tau_2}$ on both sides of Eq. (4) and taking the derivative of λ with respect to τ_2, we get

$$
\begin{aligned}
&\operatorname{sgn}\left[\operatorname{Re}\left(\frac{d\lambda}{d\tau_2}\right)_{\tau_2=\tau_{20}}\right]\\
&=\operatorname{sgn}\left\{\left[\operatorname{Re}\left(\frac{d\lambda}{d\tau_2}\right)^{-1}\right]_{\tau_2=\tau_{20}}\right\}\\
&=\operatorname{sgn}\left(\operatorname{Re}\left(\frac{E_{21}e^{\lambda\tau_2}+E_{24}e^{-\lambda\tau_1}-E_{22}\tau_1e^{-\lambda\tau_1}-2C_0\tau_1e^{-\lambda(2\tau_1+\tau_2)}}{C_0\lambda e^{-\lambda(2\tau_1+\tau_2)}-E_{23}\lambda e^{\lambda\tau_2}}-\frac{\tau_2}{\lambda}\right)_{\tau_2=\tau_{20}}\right)\\
&=\operatorname{sgn}\left(\frac{T_1T_3+T_2T_4}{{T_1}^2+{T_2}^2}\right),
\end{aligned}
$$

where

$$
\begin{aligned}
E_{21}=&4\lambda^3+3A_3\lambda^2+2A_2\lambda+A_1,\\
E_{22}=&B_2\lambda^2+B_1\lambda+B_0,\\
E_{23}=&\lambda^4+A_3\lambda^3+A_2\lambda^2+A_1\lambda+A_0,\\
E_{24}=&2B_2\lambda+B_1,\\
T_1=&\cos(\tau_1\omega_{20})\left(B_1-B_0\tau_1+B_2\tau_1\omega_{20}^2\right)+\cos(\tau_1\omega_{20})\left(A_1-3A_3\omega_{20}^2\right)\\
&-2\tau_1C_0\cos((2\tau_1+\tau_2)\omega_{20})+\omega_{20}sin(\tau_1\omega_{20})(2B_2-\tau_1B_1)\\
&+sin(\tau_{20}\omega_{20})\left(4\omega_{20}^3-2A_2\omega_{20}\right),\\
T_2=&(2B_2\omega_{20}-\tau_1B_1)\cos(\tau_1\omega_{20})+\left(2A_2\omega_{20}-4\omega_{20}^3\right)\cos(\tau_{20}\omega_{20})\\
&+\left(B_0\tau_1-B_1-\tau_1B_2\omega_{20}^2\right)sin(\tau_1\omega_{20})+\left(A_1-3A_3\omega_{20}^2\right)sin(\tau_{20}\omega_{20})\\
&+2\tau_1C_0sin((2\tau_1+\tau_2)\omega_{20}),\\
T_3=&\left(A_1\omega_{20}^2-A_3\omega_{20}^4\right)\cos(\tau_{20}\omega_{20})+\left(A_0\omega_{20}-A_2\omega_{20}^3+\omega_{20}^5\right)sin(\tau_{20}\omega_{20})\\
&+C_0\omega_{20}sin((2\tau_1+\tau_2)\omega_{20}),\\
T_4=&\left(A_2\omega_{20}^3-A_0\omega_{20}-\omega_{20}^5\right)\cos(\tau_{20}\omega_{20})+C_0\omega_{20}\cos((2\tau_1+\tau_2)\omega_{20})\\
&+\left(A_1\omega_{20}^2-A_3\omega_{20}^4\right)sin(\tau_{20}\omega_{20}).
\end{aligned}
$$

If condition (H7) $T_1T_3+T_2T_4\neq 0$ holds, then $\operatorname{Re}\left(\frac{d\lambda(\tau)}{d\tau_2}\right)^{-1}_{\tau_2=\tau_{20}}\neq 0$.

By the discussion above, we get the following theorem.

Theorem 3 *For system (1), $\tau_2>0$, $\tau_1\in[0,\tau_{10})$, and $\tau_1\neq\tau_2$. If conditions (H1),(H6) and (H7) hold, then the positive equilibrium E_* of system (1) is locally asymptotically stable when $0\leq\tau_2<\tau_{20}$ and unstable when $\tau_2>\tau_{20}$. Furthermore, system (1) undergoes a Hopf bifurcation at E_* when $\tau_2=\tau_{20}$.*

For the case $\tau_1>0$, $\tau_2\in[0,\tau_{20})$, and $\tau_1\neq\tau_2$, we can obtain similar results as those in Theorem 3.

3 Direction and Stability of Hopf Bifurcation

In this section, we consider the direction and stability of Hopf bifurcation with respect to τ_2 and $\tau_1 \in [0, \tau_{10})$ by using the methods in Hassard et al. (1981). Without loss of generality, we assume system (2) undergoes a Hopf bifurcation at $\tau_2 = \tau_{20}, \tau_1 \in [0, \tau_{10})$. For convenience, letting $\bar{u}_i(t) = u_i(\tau t), i = 1, 2, 3, \tau_2 = \tau_{20} + \mu, \mu \in R$ and dropping the bars, then system (2) becomes a functional differential equation in $C = C^1\left([-1, 0], R^3\right)$:

$$\dot{u}(t) = L_\mu u_t(\theta) + f(\mu, u_t(\theta))$$

where $u(t) = (u_1(t), u_2(t), u_3(t), u_4(t))^T$, $u_t(\theta) = u(t + \theta)(\theta \in [-\tau, 0]$ for $\theta \in [-\tau, 0]$, and $L_\mu : C \to R$, $f : R \times C \to R$ are given, respectively, by

$$L_\mu(\varphi) = (\tau_{20} + \mu)\hat{A}\varphi(0) + (\tau_{20} + \mu)\hat{B}\varphi\left(-\frac{\tau_1}{\tau_{20}}\right) + (\tau_{20} + \mu)\hat{C}\varphi(-1)$$

and

$$f(\mu, u_t(\theta)) = (\tau_{20} + \mu)(f_1, f_2, f_3)^T,$$

here

$$\hat{A} = \begin{bmatrix} a_{11} & 0 & 0 & 0 \\ 0 & a_{22} & 0 & 0 \\ 0 & 0 & a_{33} & 0 \\ 0 & 0 & 0 & a_{44} \end{bmatrix}, \quad \hat{B} = \begin{bmatrix} 0 & 0 & 0 & 0 \\ 0 & 0 & 0 & 0 \\ a_{31} & 0 & 0 & 0 \\ 0 & a_{42} & 0 & 0 \end{bmatrix},$$

$$\hat{C} = \begin{bmatrix} 0 & 0 & a_{13} & a_{14} \\ 0 & 0 & a_{23} & a_{24} \\ 0 & 0 & 0 & 0 \\ 0 & 0 & 0 & 0 \end{bmatrix},$$

$$\varphi(\theta) = (\varphi_1(\theta), \varphi_2(\theta), \varphi_3(\theta), \varphi_4(\theta))^T \in C,$$

$$f_1 = k_{11}\varphi_3^2(-1) + k_{12}\varphi_4^2(-1) + k_{13}\varphi_3^3(-1) + k_{14}\varphi_4^3(-1),$$

$$f_2 = k_{21}\varphi_3^2(-1) + k_{22}\varphi_4^2(-1) + k_{23}\varphi_3^3(-1) + k_{24}\varphi_4^3(-1),$$

$$f_3 = 0,$$

$$f_4 = 0,$$

$$k_{11} = -\frac{aa_{11}n\left(\left(P_1^*\right)^{2n-2}s^n(n+1) + \left(P_1^*\right)^{n-2}s^{2n}(1-n)\right)}{\left(s^n + \left(P_1^*\right)^n\right)^3},$$

$$k_{12} = -\frac{bb_{21}n\left(\left(P_2^*\right)^{2n-2}s^n(n+1) + \left(P_2^*\right)^{n-2}s^{2n}(1-n)\right)}{\left(s^n + \left(P_2^*\right)^n\right)^3},$$

$$k_{21} = -\frac{an\left(\left(P_2^*\right)^{2n-2}s^n\,(n+1)+\left(P_2^*\right)^{n-2}s^{2n}\,(1-n)\right)}{\left(s^n+\left(P_2^*\right)^n\right)^3},$$
$$k_{22} = -\frac{bn\left(\left(P_1^*\right)^{2n-2}s^n\,(n+1)+\left(P_1^*\right)^{n-2}s^{2n}\,(1-n)\right)}{\left(s^n+\left(P_1^*\right)^n\right)^3}.$$

By the Riesz representation theorem, there exists a matrix function $\eta(\theta,\mu),\theta\in[-1,0]$, such that

$$L_\mu(\varphi)=\int_{-1}^{0}d\eta(\theta,\mu)\varphi(\theta),\ \varphi\in C^1\left([-1,0],R^3\right).$$

Here, we choose

$$\eta(\theta,\mu)=\begin{cases}(\tau_{20}+\mu)\left(\hat{A}+\hat{B}+\hat{C}\right),\theta\in 0,\\ (\tau_{20}+\mu)\left(\hat{B}+\hat{C}\right),\theta\in\left[-\frac{\tau_1}{\tau_{20}},0\right),\\ (\tau_{20}+\mu)\hat{C},\ \theta\in\left(-1,-\frac{\tau_1}{\tau_{20}}\right),\\ 0,\ \theta=-1.\end{cases}$$

For $\varphi\in C^1\left([-1,0],R^3\right)$, define

$$A_\mu(\varphi)=\begin{cases}\frac{d\varphi(\theta)}{d\theta},\ -1\le\theta<0,\\ \int_{-1}^{0}d\eta(\theta,\mu)\varphi(\theta),\ \theta=0,\end{cases}$$

and

$$R_\mu(\varphi)=\begin{cases}\left(0\ 0\ 0\right)^T,\ -1\le\theta<0,\\ f\left(\mu,\varphi\right),\ \theta=0.\end{cases}$$

For $\psi\in C^1\left([0,1],(R^3)^*\right)$, the adjoint operator A^* of A is defined by

$$A^*(\mu)\psi=\begin{cases}-\frac{d\psi(s)}{ds},\ 0<s\le 1,\\ \int_{-1}^{0}d\eta^T(s,\mu)\psi(-s),\ s=0.\end{cases}$$

Next, we define a bilinear form:

$$\langle\psi(s),\varphi(\theta)\rangle=\bar{\psi}(0)\varphi(0)-\int_{-1}^{0}\int_{\xi=0}^{\theta}\bar{\psi}(\xi-\theta)d\eta(\theta)\varphi(\xi)d\xi,$$

where $\eta(\theta)=\eta(\theta,0)$.

Through the discussion in Sect. 2, we know $\pm i\tau_{20}\omega_{20}$ are eigenvalues of $A(0)$. They are also eigenvalues of A^*. In the following, we compute the eigenvectors of $A(0)$ and A^* corresponding to $i\tau_{20}\omega_{20}$ and $-i\tau_{20}\omega_{20}$, respectively. Assume $q(\theta) = (1, \alpha, \beta, \gamma)^{\mathrm{T}} e^{i\tau_{20}\omega_{20}\theta}$, $\theta \in [-1, 0]$ is eigenvector of $A(0)$. Then, we know

$$A(0)q(0) = i\tau_{20}\omega_{20}q(0).$$

That is,

$$\tau_{20}\begin{bmatrix} i\omega_{20} - a_{11} & 0 & -a_{13}e^{-i\tau_{20}\omega_{20}} & -a_{14}e^{-i\tau_{20}\omega_{20}} \\ 0 & i\omega_{20} - a_{22} & -a_{23}e^{-i\tau_{20}\omega_{20}} & -a_{24}e^{-i\tau_{20}\omega_{20}} \\ -a_{31}e^{-i\tau_1\omega_{20}} & 0 & i\omega_{20} - a_{33} & 0 \\ 0 & -a_{42}e^{-i\tau_1\omega_{20}} & 0 & i\omega_{20} - a_{44} \end{bmatrix} q(0) = \begin{bmatrix} 0 \\ 0 \\ 0 \\ 0 \end{bmatrix}.$$

By calculation, we get

$$q(0) = \left(1, \frac{(i\omega_{20} - a_{44})\,\Delta_1}{\Delta_2}, \frac{a_{31}e^{-i\tau_1\omega_{20}}}{i\omega_{20} - a_{33}}, \frac{a_{42}e^{-i\tau_1\omega_{20}}\Delta_1}{\Delta_2}\right)^{\mathrm{T}},$$

where

$$\Delta_1 = \frac{a_{23}a_{31}e^{-i\omega_{20}(\tau_{20}+\tau_1)}}{i\omega_{20} - a_{33}}, \Delta_2 = (i\omega_{20} - a_{44})(i\omega_{20} - a_{22}) - a_{24}a_{42}e^{-i\omega_{20}(\tau_{20}+\tau_1)}.$$

On the other hand, we assume $q^*(s) = D(1, \alpha^*, \beta^*, \gamma^*)e^{i\tau_{20}\omega_{20}s}$, $s \in [0, 1]$ is eigenvector of A^*. Thus, we have:

$$\tau_{20}\begin{bmatrix} -i\omega_{20} - a_{11} & 0 & -a_{31}e^{i\tau_1\omega_{20}} & 0 \\ 0 & -i\omega_{20} - a_{22} & 0 & -a_{42}e^{i\tau_1\omega_{20}} \\ -a_{13}e^{i\tau_{20}\omega_{20}} & -a_{23}e^{i\tau_{20}\omega_{20}} & -i\omega_{20} - a_{33} & 0 \\ -a_{14}e^{i\tau_{20}\omega_{20}} & -a_{24}e^{i\tau_{20}\omega_{20}} & 0 & -i\omega_{20} - a_{44} \end{bmatrix} \left(q^*(0)\right)^{\mathrm{T}} = \begin{bmatrix} 0 \\ 0 \\ 0 \\ 0 \end{bmatrix}.$$

It is not hard to get

$$q^*(0) = D(1, \alpha^*, \beta^*, \gamma^*) = D(1, \Delta_3, -\frac{i\omega_{20} + a_{11}}{a_{31}e^{i\tau_1\omega_{20}}}, -\frac{(i\omega_{20} + a_{22})\,\Delta_3}{a_{42}e^{i\tau_1\omega_{20}}})$$

where

$$\Delta_3 = \frac{a_{13}}{a_{23}} - \frac{(i\omega_{20} + a_{11})(i\omega_{20} + a_{33})}{a_{23}a_{31}e^{i\omega_{20}(\tau_1+\tau_{20})}}.$$

Next, normalizing q and q^* by the condition $\langle q^*, q\rangle = 1$, $\langle q^*, \bar{q}\rangle = 0$. In order to obtain $\langle q^*(s), q(\theta)\rangle = 1$, it is necessary to compute the value of D.

$$\left\langle q^*(s), q(\theta)\right\rangle$$

$$
\begin{aligned}
&= \bar{q}^*(0)\cdot q(0) - \int_{\theta=-1}^{0}\int_{\xi=0}^{\theta} \bar{q}^*(\xi-\theta)d\eta(\theta)\, q(\xi)\, d\xi \\
&= \bar{D}\left(1,\bar{\alpha}^*,\bar{\beta}^*,\bar{\gamma}^*\right)(1,\alpha,\beta,\gamma)^{\mathrm{T}} \\
&\quad - \int_{-1}^{0}\int_{\xi=0}^{\theta} \bar{D}\left(1,\bar{\alpha}^*,\bar{\beta}^*,\bar{\gamma}^*\right)e^{-i(\xi-\theta)\tau_{20}\omega_{20}}d\eta(\theta)\,(1,\alpha,\beta,\gamma)^{\mathrm{T}}e^{i\xi\tau_{20}\omega_{20}}d\xi \\
&= \bar{D}\{1+\alpha\bar{\alpha}^*+\beta\bar{\beta}^*+\gamma\bar{\gamma}^* \\
&\quad - \int_{-1}^{0}\left(1,\bar{\alpha}^*,\bar{\beta}^*,\bar{\gamma}^*\right)\theta e^{i\theta\tau_{20}\omega_{20}}d\eta(\theta)\,(1,\alpha,\beta,\gamma)^{\mathrm{T}}\} \\
&= \bar{D}\{1+\alpha\bar{\alpha}^*+\beta\bar{\beta}^*+\gamma\bar{\gamma}^*+\tau_1\left(a_{31}\bar{\beta}^*+\alpha a_{42}\bar{\gamma}^*\right)e^{-i\tau_1\omega_{20}} \\
&\quad + \tau_{20}\left(\beta\left(a_{13}+a_{23}\bar{\alpha}^*\right)+\gamma\left(a_{14}+a_{24}\bar{\alpha}^*\right)\right)e^{-i\tau_{20}\omega_{20}}\},
\end{aligned}
$$

here, we choose

$$D = \frac{1}{m+n}$$

such that $\langle q^*(s), q(\theta)\rangle = 1$, $\langle q^*(s), \bar{q}(\theta)\rangle = 0$, where $m = 1+\bar{\alpha}\alpha^*+\bar{\beta}\beta^*+\bar{\gamma}\gamma^*+\tau_1(a_{31}\beta^*+\alpha a_{42}\gamma^*)e^{i\tau_1\omega_{20}}$, $n = \tau_{20}\left(\beta\left(a_{13}+a_{23}\alpha^*\right)+\gamma\left(a_{14}+a_{24}\alpha^*\right)\right)e^{i\tau_{20}\omega_{20}}$.

Next, we employ a computation process similar to Wang et al. (2019), Deng et al. (2014), Wang and Yang (2018) to compute the coefficients as follows,

$$
\begin{aligned}
g_{20} =& 2\tau_{20}\bar{D}\left(k_{11}\beta^2+k_{12}\gamma^2+\alpha^*\left(k_{21}\beta^2+k_{22}\gamma^2\right)\right)e^{-2\tau_{20}\omega_{20}i}, \\
g_{11} =& 2\tau_{20}\bar{D}\left(k_{11}|\beta|^2+k_{12}|\gamma|^2+\alpha^*\left(k_{21}|\beta|^2+k_{22}|\gamma|^2\right)\right), \\
g_{02} =& 2\tau_{20}\bar{D}\left(k_{11}\bar{\beta}^2+k_{12}\bar{\gamma}^2+\alpha^*\left(k_{21}\bar{\beta}^2+k_{22}\bar{\gamma}^2\right)\right)e^{2\tau_{20}\omega_{20}i}, \\
g_{21} =& \tau_{20}\bar{D}[k_{11}M_1+k_{12}M_2+k_{13}M_3+k_{14}M_4 \\
&+\alpha^*\left(k_{21}M_1+k_{22}M_2+k_{23}M_3+k_{24}M_4\right).
\end{aligned}
$$

where

$$
\begin{aligned}
M_1 &= 2\beta W_{11}^{(3)}(-1)e^{-\tau_{20}\omega_{20}i}+\bar{\beta}W_{20}^{(3)}(-1)e^{\tau_{20}\omega_{20}i}, \\
M_2 &= 2\gamma W_{11}^{(4)}(-1)e^{-\tau_{20}\omega_{20}i}+\bar{\gamma}W_{20}^{(4)}(-1)e^{\tau_{20}\omega_{20}i}, \\
M_3 &= 3\beta^2\bar{\beta}e^{-\tau_{20}\omega_{20}i}, \\
M_4 &= 3\gamma^2\bar{\gamma}e^{-\tau_{20}\omega_{20}i}.
\end{aligned}
$$

The coefficients g_{20}, g_{11} and g_{02} can be computed when the parameters and delay are determined in system (1), while the coefficient g_{21} cannot be obtained since there are $W_{11}(\theta)$ and $W_{20}(\theta)$ in g_{21}. Next, we employ a calculation process similar to Wang et al. (2019), Deng et al. (2014), Wang and Yang (2018) to compute $W_{11}(\theta)$ and $W_{20}(\theta)$ as follows

$$W_{20}(\theta) = \frac{ig_{20}}{\tau_{20}\omega_{20}} q(0) e^{i\tau_{20}\omega_{20}\theta} + \frac{i\bar{g}_{02}}{3\tau_{20}\omega_{20}} \bar{q}(0) e^{-i\tau_{20}\omega_{20}\theta} + E_1 e^{2i\tau_{20}\omega_{20}\theta},$$
$$W_{11}(\theta) = \frac{-ig_{11}}{\tau_{20}\omega_{20}} q(0) e^{i\tau_{20}\omega_{20}\theta} + \frac{i\bar{g}_{11}}{\tau_{20}\omega_{20}} \bar{q}(0) e^{-i\tau_{20}\omega_{20}\theta} + E_2,$$

where $E_1 = \left(E_1^{(1)}, E_1^{(2)}, E_1^{(3)}, E_1^{(4)}\right)^{\mathrm{T}}$, $E_2 = \left(E_2^{(1)}, E_2^{(2)}, E_2^{(3)}, E_2^{(4)}\right)^{\mathrm{T}}$ can be obtained by the following equations, respectively.

$$\begin{bmatrix} 2i\omega_{20} - a_{11} & 0 & -a_{13}e^{-\tau_{20}\omega_{20}i} & -a_{14}e^{-\tau_{20}\omega_{20}i} \\ 0 & 2i\omega_{20} - a_{22} & -a_{23}e^{-\tau_{20}\omega_{20}i} & -a_{24}e^{-\tau_{20}\omega_{20}i} \\ -a_{31}e^{-\tau_1\omega_{20}i} & 0 & 2i\omega_{20} - a_{33} & 0 \\ 0 & -a_{42}e^{-\tau_1\omega_{20}i} & 0 & 2i\omega_{20} - a_{44} \end{bmatrix} E_1 = 2 \begin{bmatrix} R_1 \\ R_2 \\ 0 \\ 0 \end{bmatrix},$$
$$\begin{bmatrix} a_{11} & 0 & a_{13} & a_{14} \\ 0 & a_{22} & a_{23} & a_{24} \\ a_{31} & 0 & a_{33} & 0 \\ 0 & a_{42} & 0 & a_{44} \end{bmatrix} E_2 = -2 \begin{bmatrix} k_{11}|\beta|^2 + k_{12}|\gamma|^2 \\ k_{21}|\beta|^2 + k_{22}|\gamma|^2 \\ 0 \\ 0 \end{bmatrix}.$$

where $R_1 = \left(k_{11}\beta^2 + k_{12}\gamma^2\right) e^{-2\tau_{20}\omega_{20}i}$, $R_2 = \left(k_{21}\beta^2 + k_{22}\gamma^2\right) e^{-2\tau_{20}\omega_{20}i}$.

Thus, we obtain

$$E_1^{(1)} = \frac{2}{E} \begin{vmatrix} \left(k_{11}\beta^2 + k_{12}\gamma^2\right) e^{-2\tau_{20}\omega_{20}i} & 0 & -a_{13}e^{-\tau_{20}\omega_{20}i} & -a_{14}e^{-\tau_{20}\omega_{20}i} \\ \left(k_{21}\beta^2 + k_{22}\gamma^2\right) e^{-2\tau_{20}\omega_{20}i} & 2i\omega_{20} - a_{22} & -a_{23}e^{-\tau_{20}\omega_{20}i} & -a_{24}e^{-\tau_{20}\omega_{20}i} \\ 0 & 0 & 2i\omega_{20} - a_{33} & 0 \\ 0 & -a_{42}e^{-\tau_1\omega_{20}i} & 0 & 2i\omega_{20} - a_{44} \end{vmatrix},$$
$$E_1^{(2)} = \frac{2}{E} \begin{vmatrix} 2i\omega_{20} - a_{11} & \left(k_{11}\beta^2 + k_{12}\gamma^2\right) e^{-2\tau_{20}\omega_{20}i} & -a_{13}e^{-\tau_{20}\omega_{20}i} & -a_{14}e^{-\tau_{20}\omega_{20}i} \\ 0 & \left(k_{21}\beta^2 + k_{22}\gamma^2\right) e^{-2\tau_{20}\omega_{20}i} & -a_{23}e^{-\tau_{20}\omega_{20}i} & -a_{24}e^{-\tau_{20}\omega_{20}i} \\ -a_{31}e^{-\tau_1\omega_{20}i} & 0 & 2i\omega_{20} - a_{33} & 0 \\ 0 & 0 & 0 & 2i\omega_{20} - a_{44} \end{vmatrix},$$
$$E_1^{(3)} = \frac{2}{E} \begin{vmatrix} 2i\omega_{20} - a_{11} & 0 & \left(k_{11}\beta^2 + k_{12}\gamma^2\right) e^{-2\tau_{20}\omega_{20}i} & -a_{14}e^{-\tau_{20}\omega_{20}i} \\ 0 & 2i\omega_{20} - a_{22} & \left(k_{21}\beta^2 + k_{22}\gamma^2\right) e^{-2\tau_{20}\omega_{20}i} & -a_{24}e^{-\tau_{20}\omega_{20}i} \\ -a_{31}e^{-\tau_1\omega_{20}i} & 0 & 0 & 0 \\ 0 & -a_{42}e^{-\tau_1\omega_{20}i} & 0 & 2i\omega_{20} - a_{44} \end{vmatrix},$$
$$E_1^{(4)} = \frac{2}{E} \begin{vmatrix} 2i\omega_{20} - a_{11} & 0 & -a_{13}e^{-\tau_{20}\omega_{20}i} & \left(k_{11}\beta^2 + k_{12}\gamma^2\right) e^{-2\tau_{20}\omega_{20}i} \\ 0 & 2i\omega_{20} - a_{22} & -a_{23}e^{-\tau_{20}\omega_{20}i} & \left(k_{21}\beta^2 + k_{22}\gamma^2\right) e^{-2\tau_{20}\omega_{20}i} \\ -a_{31}e^{-\tau_1\omega_{20}i} & 0 & 2i\omega_{20} - a_{33} & 0 \\ 0 & -a_{42}e^{-\tau_1\omega_{20}i} & 0 & 0 \end{vmatrix}.$$

where

$$E=\begin{vmatrix} 2i\omega_{20}-a_{11} & 0 & -a_{13}e^{-\tau_{20}\omega_{20}i} & -a_{14}e^{-\tau_{20}\omega_{20}i} \\ 0 & 2i\omega_{20}-a_{22} & -a_{23}e^{-\tau_{20}\omega_{20}i} & -a_{24}e^{-\tau_{20}\omega_{20}i} \\ -a_{31}e^{-\tau_1\omega_{20}i} & 0 & 2i\omega_{20}-a_{33} & 0 \\ 0 & -a_{42}e^{-\tau_1\omega_{20}i} & 0 & 2i\omega_{20}-a_{44} \end{vmatrix}.$$

Similarly, we get

$$E_2^{(1)}=\frac{-2}{F}\begin{vmatrix} k_{11}|\beta|^2+k_{12}|\gamma|^2 & 0 & a_{13} & a_{14} \\ k_{21}|\beta|^2+k_{22}|\gamma|^2 & a_{22} & a_{23} & a_{24} \\ 0 & 0 & a_{33} & 0 \\ 0 & a_{42} & 0 & a_{44} \end{vmatrix},$$

$$E_2^{(2)}=\frac{-2}{F}\begin{vmatrix} a_{11} & k_{11}|\beta|^2+k_{12}|\gamma|^2 & a_{13} & a_{14} \\ 0 & k_{21}|\beta|^2+k_{22}|\gamma|^2 & a_{23} & a_{24} \\ a_{31} & 0 & a_{33} & 0 \\ 0 & 0 & 0 & a_{44} \end{vmatrix},$$

$$E_2^{(3)}=\frac{-2}{F}\begin{vmatrix} a_{11} & 0 & k_{11}|\beta|^2+k_{12}|\gamma|^2 & a_{14} \\ 0 & a_{22} & k_{21}|\beta|^2+k_{22}|\gamma|^2 & a_{24} \\ a_{31} & 0 & 0 & 0 \\ 0 & a_{42} & 0 & a_{44} \end{vmatrix},$$

$$E_2^{(4)}=\frac{-2}{F}\begin{vmatrix} a_{11} & 0 & a_{13} & k_{11}|\beta|^2+k_{12}|\gamma|^2 \\ 0 & a_{22} & a_{23} & k_{21}|\beta|^2+k_{22}|\gamma|^2 \\ a_{31} & 0 & a_{33} & 0 \\ 0 & a_{42} & 0 & 0 \end{vmatrix},$$

where

$$F=\begin{vmatrix} a_{11} & 0 & a_{13} & a_{14} \\ 0 & a_{22} & a_{23} & a_{24} \\ a_{31} & 0 & a_{33} & 0 \\ 0 & a_{42} & 0 & a_{44} \end{vmatrix}.$$

Hence, we can compute g_{21}. Further, we have the following quantities:

$$\begin{cases} c_1(0) = \frac{i}{2\tau_{20}\omega_{20}}\left(g_{11}g_{20} - 2|g_{11}|^2 - \frac{|g_{02}|^2}{3}\right) + \frac{g_{21}}{2}, \\ \mu_2 = -\frac{\mathrm{Re}\{c_1(0)\}}{\mathrm{Re}\{\lambda'(\tau_{20})\}}, \\ \beta_2 = 2\,\mathrm{Re}\{c_1(0)\}, \\ T_2 = -\frac{\mathrm{Im}\{c_1(0)\}+\mu_2\,\mathrm{Im}\{\lambda'(\tau_{20})\}}{\tau_{20}\omega_{20}}. \end{cases}$$

In summary, we have the following results.

Theorem 4 *For system (1), the following results hold.*

(i) *The sign of μ_2 determines the direction of Hopf bifurcation: Hopf bifurcation is supercritical (subcritical)if $\mu_2 > 0(\mu_2 < 0)$;*
(ii) *The sign of β_2 determines the stability of the bifurcating periodic solutions: The periodic solutions are orbitally stable (unstable) if $\beta_2 < 0$ ($\beta_2 > 0$);*
(iii) *The sign of T_2 determines the period of bifurcating periodic solutions: The period increases (decreases) if $T_2 > 0$ ($T_2 < 0$).*

4 Numerical Simulations

In this section, numerical simulations are given to illustrate the analytical results we obtained. We chose parameter $r_1 = 1, r_2 = 1, c_1 = 2, c_2 = 2, s = 0.5, a = 0.5, b = 0.5, d_1 = 2, d_2 = 2, n = 3, a_1 = 1, b_{21} = 1$ Xi and Turcotte (2015); then, system (1) becomes:

$$\begin{cases} M'_1(t) = -M_1(t) + 0.5\frac{P_1^3(t-\tau_2)}{0.5^3+P_1^3(t-\tau_2)} + 0.5\frac{0.5^3}{0.5^3+P_2^3(t-\tau_2)}, \\ M'_2(t) = -M_2(t) + 0.5\frac{P_2^3(t-\tau_2)}{0.5^3+P_2^3(t-\tau_2)} + 0.5\frac{0.5^3}{0.5^3+P_1^3(t-\tau_2)}, \\ P'_1(t) = -2P_1(t) + 2M_1(t-\tau_1), \\ P'_2(t) = -2P_2(t) + 2M_2(t-\tau_1). \end{cases} \tag{27}$$

By computation, it can be concluded that system (27) has three positive equilibrium points E_1, E_2 and E_3, where E_1 (0.931827, 0.068173, 0.931827, 0.068173) and E_3 (0.068173, 0.931827, 0.068173, 0.931827) are stable equilibrium points, and E_2 (0.5, 0.5, 0.5, 0.5) is a saddle point. System (27) will have bistable behavior. Which stable point of system (27) tends to depend on the initial values. For $\tau_1 = \tau_2 = \tau \neq 0$, we obtain $\tau_0 \approx 9.5$, the positive equilibrium points E_3 lose stability and a Hopf bifurcation occurs when the time delay τ passes through the critical value τ_0. By Theorem 2, we know system (27) is stable when $0 \leq \tau < \tau_0$, and unstable for $\tau > \tau_0$. The corresponding time cources diagram and phase portrait are depicted in Fig. 2.

When the initial value is selected near the saddle point E_2,there is no periodic solution. The stability of system (27) is maintained with time delay τ increasing (see Fig. 3).

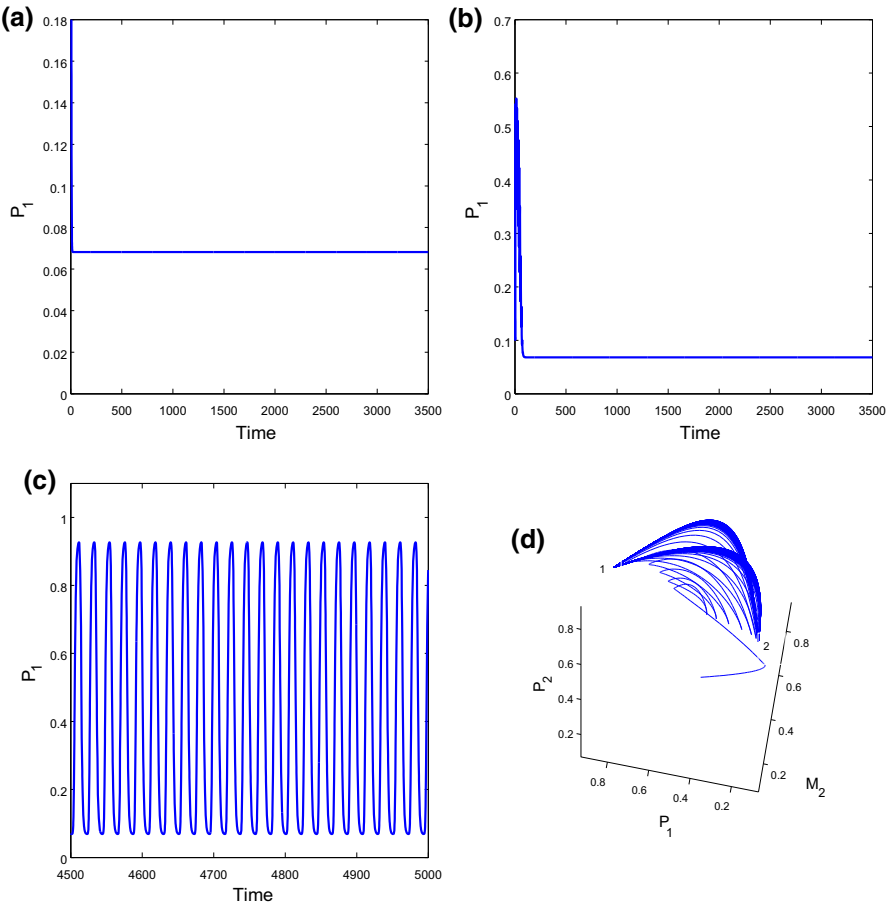

Fig. 2 Time cources diagram of P_1 and 3D phase portrait of system (27) with $\tau = 10$. **a** $\tau = 0$; **b** $\tau = 3$; **c** $\tau = 10$; **d** the delayed track oscillates between fixed point 1 and 2 that, under no-delay conditions, would be stable. Initial conditions: $M_1(0) = 0.1$, $M_2(0) = 0.35$, $P_1(0) = 0.4$, $P_2(0) = 0.3$

By computation, we can also obtain $\tau_1 = \tau_2 = \tau_0 \approx 11.5$, and a Hopf bifurcation occurs at the positive equilibrium point E_1 for $\tau = \tau_0$. By Theorem 2, we know that the positive equilibrium point E_1 of system (27) is stable when $0 \leq \tau < \tau_0$ and undergoes a Hopf bifurcation at $\tau = \tau_0 \approx 11.5$ (see Fig. 4).

Time delay can transform bistable behavior into oscillatory behavior and plays important roles in this model. Through numerical simulation, we can also draw the conclusion that the initial value and time delay both affect the dynamic behavior of system (27). With different initial values, even if the time delay is the same ($\tau_1 = \tau_2 = 67$), the trajectory of the solution of system (27) is different (see Fig. 5).

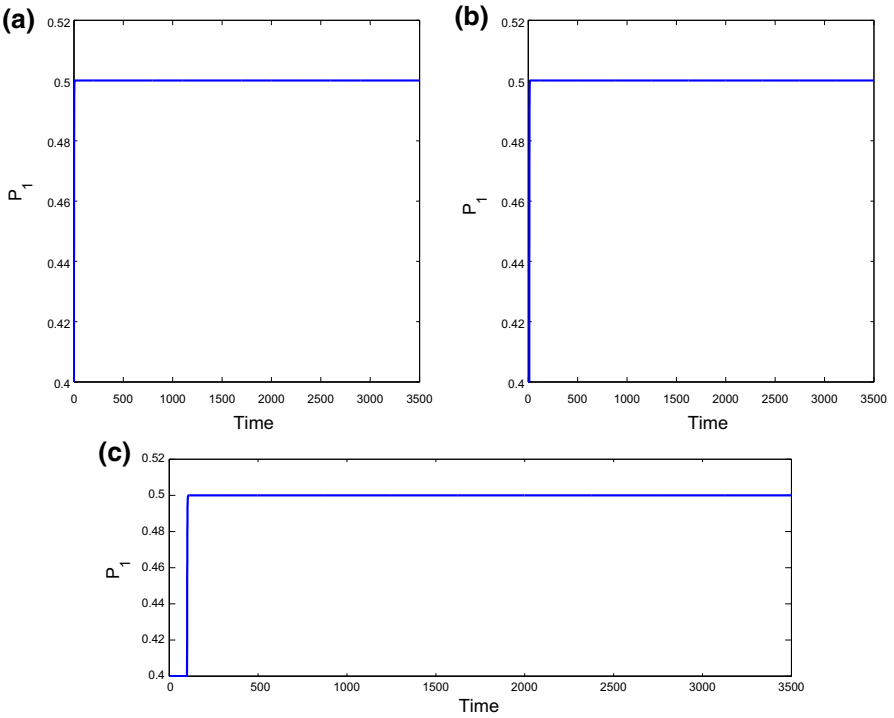

Fig. 3 Time cources diagram of P_1 with different time delay τ. **a** $\tau = 0$; **b** $\tau = 10$; **c** $\tau = 100$. Initial conditions: $M_1(0) = 0.4$, $M_2(0) = 0.4$, $P_1(0) = 0.4$, $P_2(0) = 0.4$

5 The Effect of Biological Noise

Biological systems are not purely deterministic as they comprise significant molecular noise as an often not just present but, in fact, essential component to establishing phenotype; see the general review Tsimring and Lev (2014) and Çağatay et al. (2009), Xi et al. (2013), Xi et al. (2013) for specific examples in bacteria. Here, by molecular noise, we understand biological random fluctuations of molecular components entirely due to paucity in numbers of some (or all) key species that affect the overall behavior of the system. Hence we were curious to see how our theoretical finding of the time delay-induced bifurcation to oscillations could be affected by the presence of molecular noise.

So, to this end, we used the well-traveled route provided by the Gillespie algorithm (Gillespie 1976) to translate the delayed four-dimensional deterministic model (equation #1) into a set of discrete event reactions. The detailed implementation of the stochastic algorithm for the instantaneous (no-delay) version of this system is given in Xi and Turcotte (2015). Briefly, the system was separated in a set of production and degradation reactions; each reaction corresponds to the individual production terms (positive terms) and degradation terms (negative terms) in the four differential equation system. Thus, in all, the stochastic algorithm comprises four production reactions and

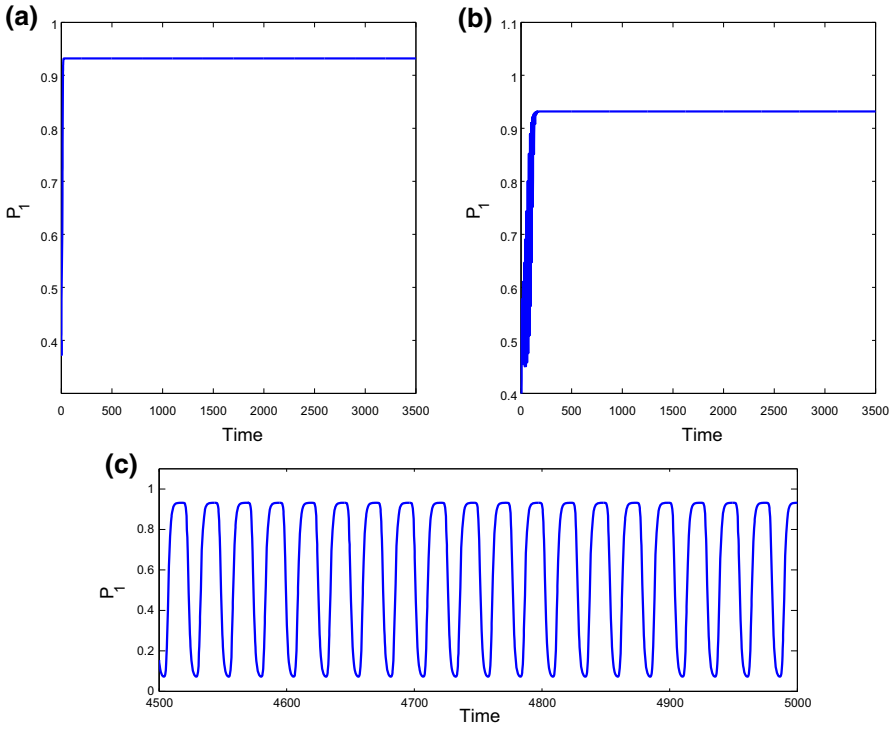

Fig. 4 Time cources diagram of P_1 with different time delay τ. **a** $\tau = 0$; **b** $\tau = 5$; **c** $\tau = 12$. Initial conditions: $M_1(0) = 0.3$, $M_2(0) = 0.35$, $P_1(0) = 0.4$, $P_2(0) = 0.3$

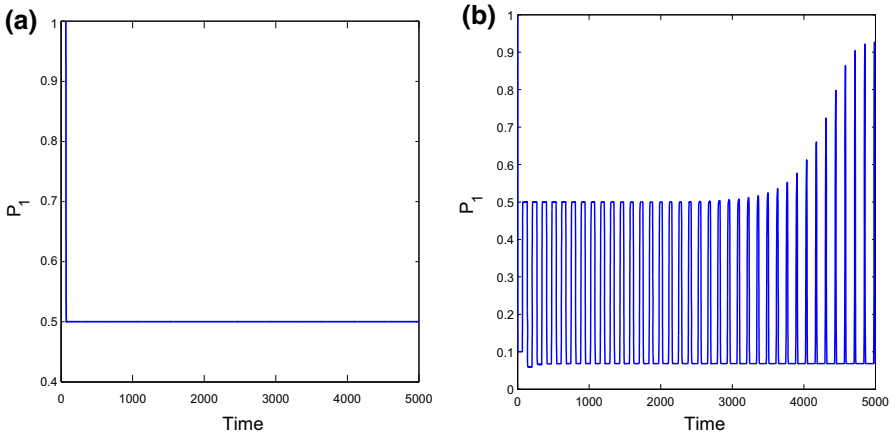

Fig. 5 Time cources diagram of P_1 with different initial conditions. **a** $M_1(0) = 1$, $M_2(0) = 1$, $P_1(0) = 1$, $P_1(0) = 1$, **b** $M_1(0) = 0.1$, $M_2(0) = 1$, $P_1(0) = 1$, $P_2(0) = 1$

four degradation reactions. Throughout the course of a stochastic simulation, reactions are individually fired according to their time-evolving propensities using the Gillespie algorithm. Stochastic simulations thus track the varying numbers of all species in the system as a function of time as discrete event reactions individually fire. Finally, the time delay is implemented by straightforward lookup into the running history of the simulation.

Figure 6 shows the result of two extended time-delayed stochastic simulations (purple and red trajectories) overlapped onto the time-delayed integration of the 4 ODE, or 4D deterministic system (cyan line). For guidance, we also show the instantaneous 2 D nullclines obtained from setting $\mathrm{dmRNA1}/\mathrm{d}t = \mathrm{dmRNA2}/\mathrm{d}t = 0$ (solid red and green lines), thus collapsing the four-dimensional system into a two-dimensional system by setting the messenger RNA sub-manifold at rest. We also show the 4D nullcline constructions (red and green circles overlapping the 2D nullclines). Actual methods on how these are computed can be found in Xi and Turcotte (2015) and would not be repeated here for brevity. The intersections of the two 2D nullclines define the locus of the 2-dimensional instantaneous system being a rest on the phase plane ($\mathrm{d}X_1/\mathrm{d}t = \mathrm{d}X_2/\mathrm{d}t = 0$). These three fixed points are labeled #1, #2 and #3. From Xi and Turcotte (2015), points #1 and #3 are stable nodes, and point #2, the middle point, is a saddle node. These fixed points are deterministic delay-free fixed points of the dynamics that we use to pin and contrast the discussion of the delayed stochastic system behavior.

First we notice that the deterministic time-delayed four-dimensional system track projected on the X_1 and X_2 plane (the cyan line) roughly oscillates between points #1 and #3. This is consistent with our earlier findings that time delay bifurcates an otherwise bistable system into an oscillatory one. The direction of rotation is counterclockwise.

Turning our attention to stochastic effects, the purple stochastic track was started at the same location on the phase plane where the deterministic track (cyan trajectory) originates. We adjusted the level of noise in the system by setting the total number of molecules per unit of concentration in the system to $\Omega = 10{,}000$. Ω actually has units of volume and is thus a convenient way to dial-in a desired noise level based on how big the sample is, while maintaining the concentrations the same. An invariant concentration is obtained by scaling both the number of molecules N_{molec} and the volume V_{system} of the system by the same factor, so the ratio $N_{\mathrm{molec}}/V_{\mathrm{system}}$ does not change. While concentrations are invariant under any Ω, the random fluctuations on these concentrations are expected to vary approximately as $1/\mathrm{sqrt}(N_{\mathrm{molec}})$. For more details the reader is referred to Tsimring and Lev (2014) and to the supplement of Çağatay et al. (2009). So, for Ω increasing, the size of the fluctuations will decrease. Because the number of molecules per unit concentration in the system is high, but not overly high, the observed fluctuations are significant, but they not overwhelming the dynamics; see Fig. 6.

The main points conveyed in Fig. 6 are twofold. Firstly, the stochastic simulation, particularly in the early phase of the purple track where the number of molecules is high, closely follows the deterministic track, even in regions of the phase space where the shape of the deterministic parent trajectory is complex. But much more importantly, secondly, in the neighborhood of point #1, we observe the purple track

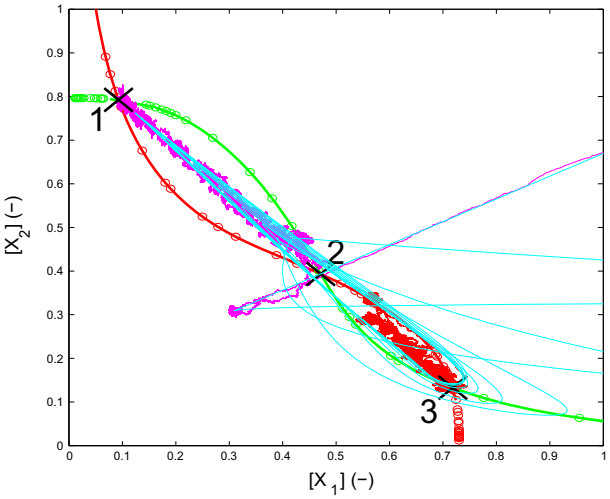

Fig. 6 Stochastic behavior. Green and red solid lines are nullclines of the instantaneous (no-delay) deterministic system, as explained in the text. Points #1, #2 and #3 are fixed points of the instantaneous system: stable, saddle and stable, respectively. The cyan line depicts the time-delayed four-dimensional system integration. The direction of rotation is counterclockwise. The purple trajectory is a delayed stochastic simulation initiated at the same starting location as the deterministic simulation (cyan line). The red trajectory is another delayed stochastic simulation, and this one initiated within the basin of attraction of point #3. Initially the red trajectory moves in the direction from 3 to 1 (as seen on the upper branch of the counterclockwise loop) but it soon hops to the lower branch, and progresses in the direction from 1 to 3. Both stochastic trajectories become trapped in the vicinity of their respective destinations (point #1 and point #3) despite the deterministic delayed systems being oscillatory (cyan line). Stochastic simulations are run with $\Omega = 10{,}000$ imparting modest noise to the system (Color figure online)

dwelling indefinitely by essentially hopping back and forth from an inward going direction to an outward going direction to point #1. We can understand how this behavior is happening because, in this region of phase space near point #1, the inward and outward flow directions are very close to each other (Fig. 6); in the pinching part of the looping track. Effectively, in vicinity of point 1, the stochastic system hops back and forth in direction inward and outward to point #1. In short, the noisy system is dynamically and stochastically trapped to the neighborhood of point 1.

The second stochastic simulation, the red track, was started closer to and in the basin of attraction of and above point #3. We see that initially this trajectory actually moves away from point #3, settling onto the outbound flow of the oscillating trajectory (upper branch of the loop). But, eventually and randomly, the stochastic system jumps back over onto the deterministic flow (lower branch of the loop) that propel deterministic tracks to move the system toward point #3. As the stochastic simulation progresses further, the inward and outward flows become closer and closer to each other on the phase plane, similar to the case of the neighborhood of point #1, described above. Hence, again, the system essentially dwells in the neighborhood of the fixed point, as it hops back and forth in direction inward and outward of point #3. Hence, the noisy system is again dynamically and stochastically trapped, but this time, to the neighborhood of point 3.

Figure 6 thus demonstrates a key and unexpected behavior imparted by molecular noise: Whereas the delayed deterministic system oscillates beyond the Hopf as shown described earlier, the equivalent stochastic delayed system will nevertheless remain bistable because noise effectively imparts a stabilizing effect through the mechanism explained above. In short, interestingly, molecular noise actually stabilizes an otherwise oscillating system. To our knowledge, the description of this behavior is original.

We have also numerically studied two limits: $\Omega = \text{large}(100{,}000)$ and $\Omega = \text{small}(100)$. In the small Ω limit, the system is quickly overwhelmed by noise (the number of particles in the system is small) and much of the interesting dynamics is blurred away. In the large Ω system, we have verified that the stochastic system's behavior, as it approaches the so-called thermodynamic limit (Gillespie 2007), as expected more and more approximates that of the deterministic system. Large Ω simulations require many thousands of hours to perform. Data are omitted for brevity.

6 Characterization of the Orbit

In this section, we briefly consider the effect of nonlinear terms in the normal form of the orbit equation. Following the lead of Molnár et al. (2016), we see that the stability and amplitude of a limit cycle born at the Hopf bifurcation depend on the cubic term in the expansion, but further away from the bifurcation, the possibility that higher-order terms (quintic,. . .) would modify the amplitude and/or would even contribute new dynamical behavior such as a fold cannot be excluded; it depends on the details of the problem (Molnár et al. 2016, Molnár 2020). Casting the problem into normal form is beyond the scope of this paper. So in order to study this nonlinear dynamical aspect, and in order to determine its potential impact on our analysis, we generated multiple time curves of the oscillations for τ just past the Hopf bifurcation and further away from it, both for short and essentially extremely large time intervals. In all cases, the attained amplitude of oscillations and frequency is the same. The data are not included here, for the sake of saving space, but it is available for perusal if needed. We therefore conclude that, for the problem we studied, such possible buildup of nonlinear effects has no impact.

7 Discussion and Conclusions

In the first part of this paper, we study the effect of two time delays on a mutually inhibitory core gene regulation circuit. In the case of instantaneous regulation (no-delay), we expect the dynamics to be bistable. Since delays are inherent to the spatial and mechanistic regulation of cells, we focus on the influence of time delays in five special cases and thus obtain the conditions for the stability and the bifurcation of system (1) to oscillations. We derive a formula to determine the direction of the Hopf bifurcation and the stability of the periodic solutions by applying the normal form method and the center manifold theorem. In the absence of time delays, bistable behavior occurs in system (1), so the selection of initial values is very important. A separatrix passing through the middle saddle point divides the respective basins of

attraction of the two stable fixed points on either side. By adding time delay to the dynamics of the regulation, the bistable behavior can be transformed into oscillatory behavior. Delay and initial values combine to affect the dynamic behavior of the system. Thus, complex dynamic behavior appears. Numerical simulations are performed to illustrate and confirm the analytical results.

In the second part of the paper, we turned out attention to the effect of biological noise on the system. In many cases, noise could be naively expected to destabilize an otherwise stable system. But our main point in the deterministic analysis was that delays induce oscillations via Hopf bifurcation in an otherwise bistable system. The delayed system is already "unstable" through oscillations. So, what then could the effect of unavoidable biological noise on the now oscillatory system be? Somewhat un-intuitively, our numerical simulations, based on the robust Gillespie algorithm augmented to account for delays, showed that the fluctuations actually stabilize the otherwise oscillatory system. By carefully studying the developing stochastic histories, we established the mechanism for this. In fact, near destabilized fixed points of the dynamics, noise allows the delayed stochastic system to essentially hop from inward going flow to outward flow and back. Thus, noise actually re-stabilizes a de-stabilized point. Hence, while the delayed deterministic dynamics bifurcates to the present oscillatory behavior, the stochastic dynamics acts to recover bistability, in effect, negating the effects of delays.

Delays are inherent to transport and other mechanisms in the cell and are thus not only un-avoidable, but because they are part of how biological systems work, they cannot reasonably be ignored. The same is also true about fluctuations in the concentrations of molecular regulators of living systems. In this work we chose perhaps the simplest and best example there can be of a meaningful core biological control circuit—the "bistable switch"—to first demonstrate its inherent fragility to time delays under a deterministic analysis. Bistability is a dynamic feature that enables commitment to one of two possible states. But here, we explicitly show that time delays impact the behavior of the system by breaking this commitment and permitting switching back and forth between otherwise stable states. Further, and perhaps even more importantly, we show that unavoidable biological noise somewhat unintuitively restores the bistable behavior of the system.

In further work, we plan to study in more details the efficiency of the noise stabilization process for it cannot be excluded that noise may allow, with some probability, occasional exit from the re-stabilized point. And clearly the size of the noise will have an impact. We also plan to explore the impact of the number of bifurcations and of another unavoidable feature of realistic biological circuits, timescale separation, in this and particularly in other progressively more complex systems. And of course, propelled by the results we obtained in this analysis, we plan to continue the study of how biological noise impacts dynamical behavior. We expect this work to continue helping shedding light on how and particularly why Evolution selects certain gene regulation circuit topologies over others.

Acknowledgements The authors wish to express sincere thanks to anonymous referee number 2 for very valuable suggestions. ZY and WG acknowledge support from NSFC 11872084.

Compliance with ethical standards

Methods In numerical simulations, ODEs and DDEs were separately integrated by using ODE45 and DDE23 in MATLAB R2014a.

Appendix

$$
\begin{aligned}
m_0 &= 4B_0^2A_0C_0,\\
m_1 &= 2C_0\left(2B_0A_0B_1 - A_1B_0^2\right),\\
m_2 &= 4C_0\left(2A_1B_1B_0 - 2A_0B_2B_0 - A_0B_1^2 - A_1B_0^2\right),\\
m_3 &= 2C_0\left(A_3B_0^2 - 2B_2B_1A_0 - 2B_0B_1A_2 + A_1B_1^2 + 2B_0B_2A_1\right),\\
m_4 &= 4C_0\left(-2A_3B_1B_0 - 2A_1B_1B_2 + 2A_2B_2B_0 + 4B_2^2A_0 + A_2B_1^2 + B_0^2\right),\\
m_5 &= 2C_0\left(2A_2B_1B_2 - A_3B_1^2 - 2A_3B_0B_2 + 2B_1B_0 - A_1B_2^2\right),\\
m_6 &= 4C_0\left(2A_3B_1B_2 + B_2^2A_2 - B_1^2 - 2B_2B_0\right),\\
m_7 &= 2C_0\left(B_2^2A_3 - 2B_1B_2\right),\\
m_8 &= 4C_0B_2^2,\\
n_1 &= 2A_3^2 - 4A_2,\\
n_2 &= A_3^4 + 6A_2^2 - B_2^2 - 4A_1A_3 - 4A_2A_3^2 + 4A_0,\\
n_3 &= 2A_1^2 - 12A_0A_2 - 4A_2^3 + 2B_2^2A_2 - A_3^2B_2^2 + 2B_2B_0 + 4A_0A_3^2 + 8A_1A_2A_3\\
&\quad +2A_2^2A_3^2 - B_1^2 - 4A_3^3A_1,\\
n_4 &= 2B_1^2A_2 - 8A_0A_1A_3 - B_0^2 - A_3^2B_1^2 + 12A_0A_2^2 - A_2^2B_2^2 - 2C_0^2 + 6A_1^2A_3^2\\
&\quad +A_2^4 + 6A_0^2 - 2B_2^2\left(A_0 + C_0 - A_3^2B_0 - A_1A_3\right)\\
&\quad -4A_2\left(A_1A_2A_3 + B_0B_2 + A_0A_3^2 + A_1^2\right),\\
n_5 &= 4A_2C_0^2 - 12A_2A_0^2 + 2A_1^2\left(2A_0 + A_2^2\right) + 2A_3^2\left(A_0^2 - C_0^2\right) - 4A_2^3A_0\\
&\quad -A_1^2\left(4A_1A_3 + B_2^2\right)\\
&\quad +B_0^2\left(2A_2 - A_3^2\right) + B_1^2\left(2C_0 - A_2^2 - 2A_0 + 2A_1A_3\right)\\
&\quad -4A_3\left(B_1B_2C_0 + B_0B_2A_1\right)\\
&\quad +8A_0A_1A_2A_3 + 4B_0B_2\left(A_0 + C_0\right) + 2A_2B_2\left(B_2C_0 + A_2B_0\right),\\
n_6 &= 6A_2^2A_0^2 - 2C_0^2\left(2A_0 - A_2^2\right) - A_1^2B_1^2 - B_2^2\left(A_0^2 + C_0^2\right)\\
&\quad -B_0^2\left(2A_0 + 2C_0 + A_2^2\right)\\
&\quad +4B_1C_0\left(B_2A_1 + B_0A_3\right) - 4B_2\left(A_2B_0A_0 + A_2B_0C_0\right)
\end{aligned}
$$

$$
\begin{aligned}
&+2B_0B_2A_1^2+2A_1A_3B_0^2\\
&+2B_1^2A_2\left(A_0-C_0\right)-4A_0A_2A_1^2+4A_1A_3\left(C_0^2-A_0^2\right)-2A_0C_0B_2^2\\
&+4A_0^3+A_1^4,\\
n_7 &= 2B_0^2A_2C_0+2A_1^2A_0^2+2C_0^2B_0B_2-4A_1B_1B_0C_0-A_1^2\left(B_0^2+2C_0^2\right)\\
&+2B_1^2A_0C_0\\
&+4B_2A_0B_0C_0+A_0^2\left(2B_0B_2-B_1^2\right)-C_0^2\left(B_1^2-4A_0A_2\right)-4A_2A_0^3\\
&+2B_0^2A_0A_2,\\
n_8 &= -2B_0^2A_0C_0-A_0^2\left(2C_0^2+B_0^2\right)-B_0^2C_0^2+A_0^4+C_0^4,\\
M_1^* &= c_1P_1^*/d_1,\\
P_2^* &= \left(-bb_{21}d_1\left(s^{2n}+s^n\left(p_1^*\right)^n\right)\right)\Big/\\
&\quad\left(-r_1c_1P_1^*s^n-r_1c_1\left(P_1^*\right)^{n+1}+aa_1\left(P_1^*\right)^nd_1\right)-s^n\Big)^{(1/n)},\\
M_2^* &= c_2P_2^*/d_2.
\end{aligned}
$$

References

Bar-Or R-L, Maya R, Segel L-A, Alon U, Levine A-J, Oren M (2000) Generation of oscillations by the p53-Mdm2 feedback loop: a theoretical and experimental study. Proc Natl Acad Sci 97(21):11250–11255

Bodnar M, Bartłomiejczyk A (2012) Stability of delay induced oscillations in gene expression of Hes1 protein model. Nonlinear Anal Real World Appl 13(5):2227–2239

Çağatay T, Turcotte M, Elowitz MB et al (2009) Architecture-dependent noise discriminates functionally analogous differentiation circuits. Cell 139(3):512–522

Deng L, Wang X, Peng M (2014) Hopf bifurcation analysis for a ratio-dependent predator-prey system with two delays and stage structure for the predator. Appl Math Comput 231:214–230

Gillespie D-T (1976) A general method for numerically simulating the stochastic time evolution of coupled chemical reactions. J Comput Phys 22(4):403–434

Gillespie DT (2007) Stochastic simulation of chemical kinetics. Annu Rev Phys Chem 58(1):35–55

Hassard B-D, Kazarinoff N-D, Wan Y-H (1981) Theory and applications of Hopf bifurcation. Cambridge University Press, Cambridge

Huang B, Tian X, Liu F, Wang W (2016) Impact of time delays on oscillatory dynamics of interlinked positive and negative feedback loops. Phys Rev E 94(5):052413

Lai Q (2018) Stability and bifurcation of delayed bidirectional gene regulatory networks with negative feedback loops. Chin J Phys 56(3):1064–1073

Lewis J (2003) Autoinhibition with transcriptional delay: a simple mechanism for the zebrafish somitogenesis oscillator. Curr Biol 13(16):1398–1408

Ling G, Guan ZH, Liao R-Q, Cheng X-M (2015) Stability and bifurcation analysis of cyclic genetic regulatory networks with mixed time delays. SIAM J Appl Dyn Syst 14(1):202–220

Ling G, Guan Z-H, Hu B, Lai Q, Wu Y (2017) Multistability and bifurcation analysis of inhibitory coupled cyclic genetic regulatory networks with delays. IEEE Trans Nanobiosci 16(3):216–225

Molnár (2020) Private communication

Molnár T, Insperger T, Stépán G (2016) Analytical estimations of limit cycle amplitude for delay-differential equations. Electron J Qual Theory Differ Equ 2016(77):1–10

Monk NAM (2003) Oscillatory expression of Hes1, p53, and NF-driven by transcriptional time delays. Curr Biol 13(16):1409–1413
Parmar K, Blyuss K-B, Kyrychko Y-N, Hogan S-J (2015) Time-delayed models of gene regulatory networks. Comput Math Methods Med 2015:347273
Qiu Z (2010) The asymptotical behavior of cyclic genetic regulatory networks. Nonlinear Anal. Real World Appl. 11(2):1067–1086
Sun Q, Xiao M, Tao B (2018) Local bifurcation analysis of a fractional-order dynamic model of genetic regulatory networks with delays. Neural Process Lett 47(3):1285–1296
Suzuki Y, Lu M, Ben-Jacob E, Onuchic J-N (2016) Periodic, quasi-periodic and chaotic dynamics in simple gene elements with time delays. Sci. Rep. 6:21037
Tsimring, Lev S (2014) Noise in biology. Reports Prog Phys Phys Soc 77(2):026601
Verdugo A, Rand R (2008) Hopf bifurcation in a DDE model of gene expression. Commun Nonlinear Sci Numer Simul 13(2):235–242
Wang K, Wang L, Teng Z, Jiang H (2010) Stability and bifurcation of genetic regulatory networks with delays. Neurocomputing 73(16–18):2882–2892
Wang G, Yang Z, Turcotte M (2019) Stability and Hopf bifurcation analysis in a delayed three-node circuit involving interlinked positive and negative feedback loops. Math Biosci 310:50–64
Wang G, Yang Z (2018) Stability and Hopf bifurcation analysis in a delayed Myc/E2F/miR-17-92 network involving interlinked positive and negative feedback loops. Discrete Dyn Nat Soc 2018:7014789
Wu F-X (2011) Global and robust stability analysis of genetic regulatory networks with time-varying delays and parameter uncertainties. IEEE Trans Biomed Circuits Syst 5(4):391–398
Wu F-X (2011) Stability and bifurcation of ring-structured genetic regulatory networks with time delays. IEEE Trans Circuits Syst I Regul Pap 59(6):1312–1320
Wu X-P, Eshete M (2011) Bifurcation analysis for a model of gene expression with delays. Commun Nonlinear Sci Numer Simul 16(2):1073–1088
Xi H, Turcotte M (2015) Parameter asymmetry and time-scale separation in core genetic commitment circuits. Quant Biol 3(1):19–45
Xi H, Duan L, Turcotte M (2013) Point-cycle bistability and stochasticity in a regulatory circuit for *Bacillus subtilis* competence. Math Biosci 244(2):135–147
Xi H, Yang Z, Turcotte M (2013) Subtle interplay of stochasticity and deterministic dynamics pervades an evolutionary plausible genetic circuit for *Bacillus subtilis* competence. Math Biosci 246(1):148–163
Yue D, Guan Z-H, Chen J, Ling G, Wu Y (2017) Bifurcations and chaos of a discrete-time model in genetic regulatory networks. Nonlinear Dyn 87(1):567–586
Zhang Y, Liu H, Yan F, Zhou J (2017) Oscillatory behaviors in genetic regulatory networks mediated by microRNA with time delays and reaction–diffusion terms. IEEE Trans Nanobiosci 16(3):166–176